

# Supporting Information for

## Modifying Self-Assembled Peptide Cages to Control Internalization into Mammalian Cells

Joseph L. Beesley,<sup>†,‡</sup> Holly E. Baum,<sup>§,⊥,‡</sup> Lorna R. Hodgson,<sup>§</sup> Paul Verkade,<sup>§,||</sup> George S. Banting,<sup>\*,§</sup> and Derek N. Woolfson<sup>\*,†,§,⊥</sup>

<sup>†</sup>School of Chemistry, University of Bristol, Bristol BS8 1TS, United Kingdom

<sup>§</sup>School of Biochemistry, University of Bristol, Bristol BS8 1TD, United Kingdom

<sup>||</sup>Wolfson Bioimaging Facility, University of Bristol, Bristol BS8 1TD, United Kingdom

<sup>⊥</sup>BrisSynBio, University of Bristol, Bristol BS8 1TQ, United Kingdom

\*To correspondence shoulds be addressed: [g.banting@bristol.ac.uk](mailto:g.banting@bristol.ac.uk) and [d.n.woolfson@bristol.ac.uk](mailto:d.n.woolfson@bristol.ac.uk)

<sup>‡</sup>Contributed equally to this work.

## MATERIALS AND METHODS

### Materials

Rink amide ChemMatrix™ resin was purchased from PCAS Biomatrix Inc, Canada. Fmoc-protected amino acids, activators and dimethylformamide (DMF) were supplied by Cambridge Reagents, UK. Alexa Fluor 488 carboxylic acid, tris(triethylammonium) salt was obtained from Thermo Fisher Scientific, USA. All other chemicals were purchased from Sigma-Aldrich, UK and all additional solvents were obtained from Fisher Scientific, UK. Trypsin-EDTA (0.25 %) was purchased from Thermo Fisher Scientific, UK. Prolong Gold antifade mountant was obtained from Invitrogen, UK. XTT Cell Viability assay kit was purchased from Insight Biotechnology, UK. All other cell biology reagents were purchased from Sigma-Aldrich, UK.

### Peptide synthesis

Peptides were synthesized on a 0.1 mmol scale from Rink amide resin by standard 9-fluorenylmethoxycarbonyl (Fmoc) solid-phase peptide synthesis (SPPS) on a CEM Liberty Blue™ microwave peptide synthesizer with inline UV monitoring.<sup>1</sup> Synthesis was achieved by repeated steps of coupling (5 eq. Fmoc-amino acid, 4.5 eq. *N,N*-diisopropylcarbodiimide (DIC), 10 eq. 6-chloro-1-hydroxybenzotriazole (Cl-HOBt) in DMF, 80 °C, 5 min) and deprotection (20 % morpholine in DMF, 80 °C, 5 min) interspaced with DMF washes.

Following SPPS, peptides were *N*-terminally acetylated (acetic anhydride (3 eq.), diisopropylethylamine (DIPEA; 4.5 eq.) in DMF (10 mL), room temperature (RT), 20 min). After thorough washes with DMF and then dichloromethane (DCM), peptides were cleaved from the solid support (15 mL trifluoroacetic acid (TFA):triisopropylsilane (TIPS):H<sub>2</sub>O (38:1:1, v/v), RT, 3 h) and the resin was removed by filtration. The volume of TFA was reduced to ~ 5 mL under a positive flow of nitrogen and the crude peptide mixture was precipitated into 45 mL ice-cold diethyl ether and recovered by centrifugation (2000 x g, 4 °C, 10 min). The pellet was redissolved in ~ 10 mL MeCN:H<sub>2</sub>O (1:1, v/v) and lyophilized to yield a white solid.

Alexa Fluor 488 was coupled to the C-terminus of CC-Tri3<sup>488</sup> through the incorporation of an orthogonally protected lysine residue: Lys(alloc). The synthesized peptide was *N*-terminally acetylated and retained on the resin for Lys(alloc) deprotection and Alexa Fluor 488 coupling. To selectively remove the alloc group, the resin was washed with deoxygenated DCM (3 x 20 mL), incubated with deprotection mix (1 eq. Pd(PPh<sub>3</sub>)<sub>4</sub>, 40 eq. phenylsilane,

10 mL deoxygenated DCM, RT, 30 min), washed with DCM (3 x 20 mL), DMF (3 x 20 mL) and deoxygenated DCM (3 x 20 mL) before being incubated with fresh deprotection mix (RT, 30 min). Following this, the resin was washed with DCM (3 x 20 mL), DMF (3 x 20 mL), dioxane:H<sub>2</sub>O (9:1, v/v; 2 x 20 mL), MeOH (1 x 20 mL) and DMF (3 x 20 mL). Finally, AlexaFluor488 was coupled to the exposed primary amine (1.5 eq. AlexaFluor488, 1.35 eq. 1-[bis(dimethylamino)methylene]-1H-1,2,3-triazolo[4,5-b]pyridinium 3-oxid hexafluorophosphate (HATU), 1.5 eq. DIPEA in DMF, RT, 12 h) and the peptide cleaved as described above.

### **Peptide purification**

Crude peptide mixtures were purified to homogeneity by semi-preparative reverse-phase high-performance liquid chromatography (RP-HPLC) using a Phenomenex Luna (5 µm, 100 Å, 10 mm ID x 150 mm L) C18 reverse phase column and 0.1 % TFA in H<sub>2</sub>O (A) and 0.1 % TFA in MeCN (B) as eluents. Typically, a linear gradient of 20 % B to 80 % B was applied at a flow rate of 3 mL.min<sup>-1</sup> over 30 min. Collected fractions were analyzed by matrix-assisted laser desorption/ionisation time-of-flight (MALDI-TOF) mass spectrometry and automated analytical RP-HPLC before fractions found to contain solely the desired product were pooled and lyophilized.

### **Hub peptide formation**

Hub peptides were synthesized by asymmetric disulphide bond formation as previously described.<sup>2</sup> Briefly, the cysteine of CC-Tri3 (or a variant thereof) was activated through reaction with 2,2'-dipyridyldisulphide and purified by RP-HPLC. The activated peptide was then mixed with CC-Di-A or CC-Di-B at equimolar concentration to yield Hub-A or Hub-B (or a variant thereof), respectively and purified by RP-HPLC.

### **Circular dichroism spectroscopy**

Peptides were analyzed at 50 µM with 250 µM tris(2-carboxyethyl)phosphine (TCEP) in phosphate-buffered saline (PBS) in 1 mm pathlength quartz cuvettes using a J-810 or J-815 spectropolarimeter (JASCO, Japan) fitted with a Peltier temperature controller. Thermal denaturation experiments were performed by increasing the temperature from 5 °C to 90 °C at a linear rate of 40 °C.h<sup>-1</sup> with the circular dichroism at 222 nm recorded at 1 °C intervals. Following thermal denaturation, the sample was cooled to 5 °C and a postmelt scan was recorded to ensure refolding. All raw data were normalized for concentration, pathlength and the number of amide bonds to give mean residue ellipticity (MRE; Equation 1). Melting temperature ( $T_M$ ) was determined from the point of inflection of the thermal denaturation curve. Fraction helix values were calculated using Equation 2.<sup>3</sup>

$$MRE = \frac{\theta \cdot 0.1}{c \cdot l \cdot n}$$

**Equation 1.** Normalisation of mdeg ( $\theta$ ) to mean residue ellipticity (MRE), where  $c$  is concentration in M,  $l$  is pathlength in cm and  $n$  is the number of amide bonds.

$$\text{Fraction helix (\%)} = \frac{100 \cdot (MRE_{222} - MRE_{coil})}{\left(-42500 \cdot \left(1 - \frac{3}{n}\right)\right) - MRE_{coil}}$$

**Equation 2.** Calculation of fraction helix, where  $MRE_{coil} = 640 - 45T = 415 \text{ deg.cm}^2.\text{dmol}^{-1}.\text{bond}^{-1}$  and  $n$  is the number of amide bonds. All fraction helix values were calculated at 5 °C.

### Analytical ultracentrifugation

Sedimentation equilibrium (SE) analytical ultracentrifugation experiments were performed at 20 °C in an Optima XL-A analytical ultracentrifuge (Beckman, USA) employing an An-50 Ti rotor with Epon 6 channel centrepieces and quartz windows. Peptides were analyzed at 325  $\mu\text{M}$  with 1.63 mM TCEP in PBS. Reference channels contained 1.63 mM TCEP in PBS. Samples were centrifuged at speeds in the range of 22 – 42 krpm. Collected data was fitted to a single, ideal species model using Ultrascan II and 95 % confidence limits were calculated *via* Monte Carlo analysis of the obtained fits.

### SAGE formation

Hub peptides were dissolved in the required buffer to the desired concentration and combined for 1 h at RT to assemble SAGE particles. Hub peptide stoichiometry was controlled by changing the volume of the hub peptides added. Hub peptides of the same type (*i.e.* all Hub-A variants) were combined before final SAGE assembly.

### Scanning electron microscopy

SAGEs were assembled at 50  $\mu\text{M}$  peptide concentration in 4-(2-hydroxyethyl)-1-piperazineethanesulfonic acid (HEPES)-buffer saline (HBS; 25 mM HEPES, 150 mM NaCl, pH 7) and allowed to assemble for 1 h. 5  $\mu\text{L}$  of sample was transferred to a carbon-coated aluminium stub and allowed to air dry for 3 h before being gold-coated on a K575X sputter coater (Emitech, UK; 40 mA, 30 s). Micrographs were collected on a Quanta 200 instrument

(FEI, Netherlands) and analyzed using Fiji, a distribution of ImageJ.<sup>4</sup> Coating thickness (~5 nm) was included in particle diameter measurements.<sup>2</sup>

### **Cell biology**

Cell culture procedures were performed in a Class II microbiological safety cabinet (Thermo Scientific, UK) under sterile conditions. HeLa cells (ATCC, USA) were cultured in high glucose Dulbecco's Modified Eagle's Medium supplemented with 10 % foetal bovine serum (herein referred to as DMEM) and maintained in a CO<sub>2</sub> incubator (Thermo Scientific, UK) at 37 °C with 5 % CO<sub>2</sub> in a humidified atmosphere. Cells were detached for passaging by trypsin treatment (0.25 % v/w trypsin with 0.53 mM EDTA in Hank's Balanced Salt Solution (HBSS), 37 °C, 5 min) and the enzyme inhibited by the addition of 5 mL DMEM. Stock cells were maintained at 10 – 90 % confluence. A Nikon Eclipse TS1500 inverted light microscope (Nikon, UK) was used to visually assess cell viability and density.

### **Cytotoxicity studies**

Cell viability was assessed using the colorimetric XTT assay. HeLa cells were seeded at 6000 cells.well<sup>-1</sup> in a 96-well plate 24 h prior to experiment and incubated with samples for a further 24 h. Cells were incubated with activated XTT solution (XTT:phenazine methosulphate (200:1, v/v), 25 µL.well<sup>-1</sup>, 3 h) before absorbance was measured at 475 nm and a subtracted background reading measured at 660 nm on a CLARIOstar plate reader (BMG Labtech, USA). One-way ANOVA followed by Dunnett's multiple comparisons test was performed using GraphPad Prism version 7.00 for Windows (GraphPad Software, La Jolla California USA, [www.graphpad.com](http://www.graphpad.com)).

### **Confocal microscopy**

Cells were seeded at 2.5 x 10<sup>4</sup> cells.well<sup>-1</sup> on 9 mm glass coverslips in 48-well plate 24 h prior to experiment. Seeded cells were exposed to assembled SAGE particles (2.5 µM peptide concentration in DMEM, RT, 1 h, dark) and incubated at 37 °C with 5 % CO<sub>2</sub> for the desired time. Following SAGE exposure, cells were transferred to ice, washed once with ice-cold PBS and treated with ice-cold TCEP (5 mM in PBS, on ice, 20 min) to break down any extracellular SAGE particles (by reduction of disulfide bonds). Samples were fixed (4 % paraformaldehyde, on ice, 10 min), permeabilized (0.2 % saponin in PBS, RT, 10 min) and blocked (3 % bovine serum albumin (BSA) & 0.1 % saponin in PBS, RT, 30 min) with three ice-cold PBS washes in between each step. Cells were labeled using Alexa Fluor 594 Phalloidin (to decorate F-actin) and DAPI (nuclei) (RT, 1 h, dark) before undergoing three PBS washes. Finally, coverslips were dipped in H<sub>2</sub>O to remove any salt and mounted onto glass microscope slides (Prolong™ Gold antifade mountant, RT, 24 h, dark).

Samples were imaged on a Leica SP5-AOBS confocal laser scanning microscope attached to a Leica DMI6000 inverted epifluorescence microscope (Leica, Germany) employing a 63 x oil-immersion objective, the 488 nm line of a 100 mW Ar laser, the 594 nm line of a 2 mW Orange HeNe laser and a 50 mW 405 nm diode laser. Images were collected at a resolution of 1024 x 1024 pixels and sequential scanning was performed to prevent bleed-through between channels. Confocal images were viewed and processed using Leica LAS AF Lite software (Leica, Germany).

### Flow cytometry

Cells were seeded at  $5 \times 10^4$  cells.well<sup>-1</sup> in 48-well plates 24 h prior to experiment. Seeded cells were exposed to assembled SAGE particles (2.5  $\mu$ M peptide concentration in DMEM, RT, 1 h, dark) and incubated at 37 °C with 5 % CO<sub>2</sub> for the desired duration. Following SAGE exposure, cells were detached by Accutase treatment (200  $\mu$ L.well<sup>-1</sup>, RT, 20 min, dark), which was subsequently neutralised by DMEM addition (200  $\mu$ L.well<sup>-1</sup>). Cells were pelleted by centrifugation (100 x g, 4 °C, 4 min) and resuspended in ice-cold PBS. Samples were analyzed in the presence of 0.1 % Trypan Blue to quench all extracellular fluorescence.<sup>5</sup>

Cells were analyzed live in ice-cold PBS on a FACSCanto II (BD Biosciences, USA) employing a 488 nm laser line. Data were analyzed using Flowing software (retrieved from [flowingsoftware.btk.fi](http://flowingsoftware.btk.fi)). The percentage of SAGE positive cells was calculated by determining the percentage of cells with a fluorescence greater than the maximum fluorescence detected in the negative control (Fig. S1). Where appropriate, the percentage of SAGE positive cells against time was fitted with a logistic function (Equation 3). When fitting data represented as SAGE positive cells, A<sub>2</sub> was fixed at 100 and all other parameters floated. The geometric mean (GeoMean) is a more accurate descriptor of logarithmic data than the conventional mean and is used throughout to describe the average fluorescence intensity of a cell population. Where appropriate, these data were fitted with a fully floated logistic function (Equation 3).

$$y = \frac{A_1 - A_2}{1 + \left(\frac{x}{x_0}\right)^p} + A_2$$

**Equation 3.** Logistic function used to fit flow cytometry data. A<sub>1</sub> and A<sub>2</sub> represent lower and upper limits of the fit respectively, x<sub>0</sub> is the x value at which y = (A<sub>1</sub>+A<sub>2</sub>)/2 and p represents the gradient of the tangent to the curve at x = x<sub>0</sub>.

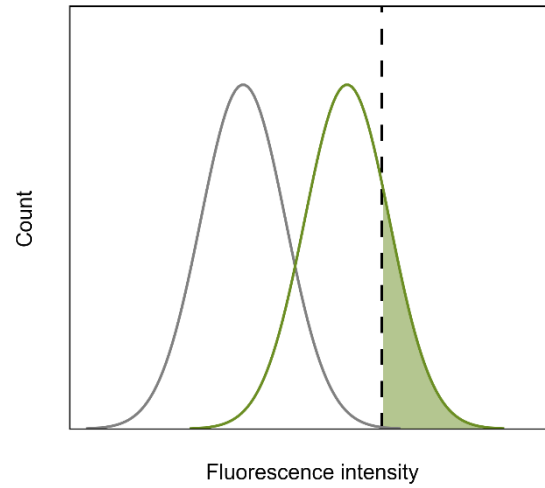


**Figure S1.** Schematic showing the calculation of SAGE-positive cells from flow cytometry data. The percentage of the cell population (green) displaying a greater fluorescence than the maximum (dashed line) of the negative control population (grey) is deemed SAGE-positive (green shaded).

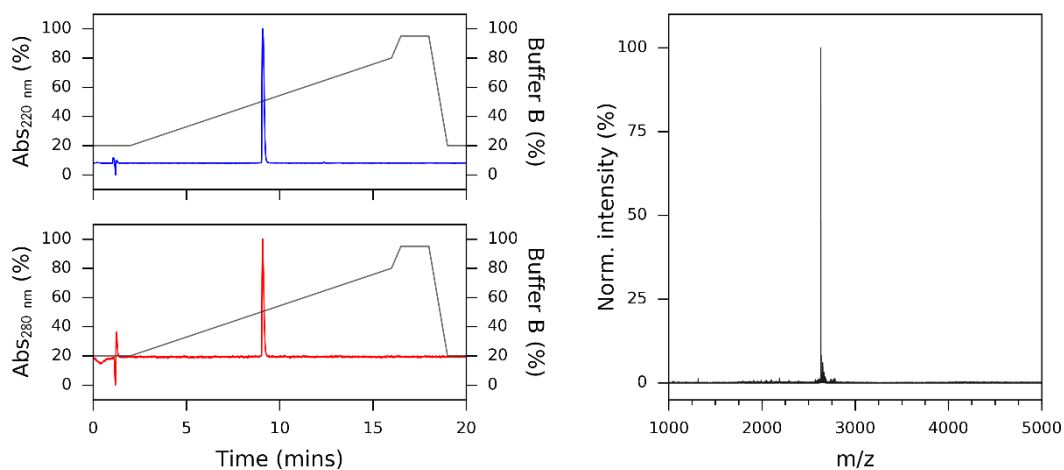


**Figure S2a.** CC-Tri3 HPLC (left; 220 and 280 nm) and MALDI-TOF MS spectra (right).  
Calculated mass = 2630.15 Da, observed mass = 2630.77 Da.

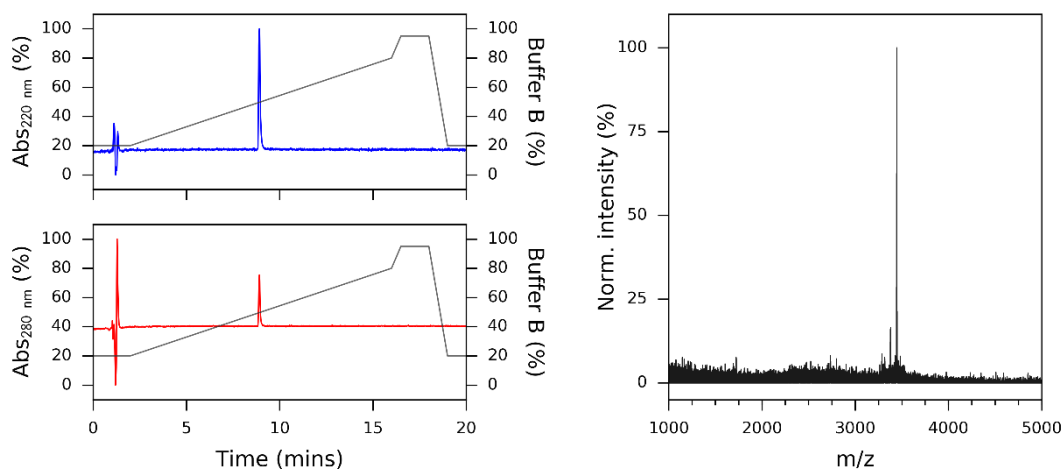


**Figure S2b.** CC-Tri3<sup>488</sup> HPLC (left; 220 and 280 nm) and MALDI-TOF MS spectra (right).  
Calculated mass = 3443.92 Da, observed mass = 3444.61 Da.

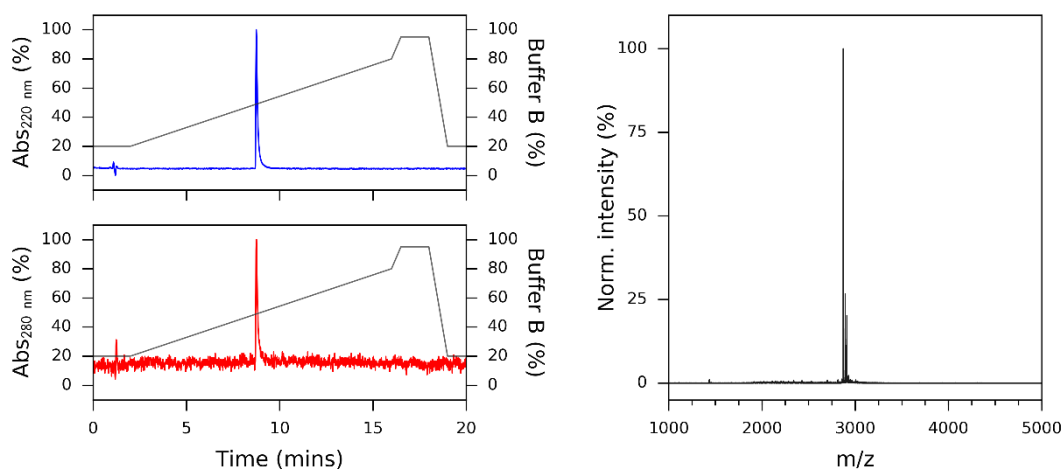


**Figure S2c.** K1-CC-Tri3 HPLC (left; 220 and 280 nm) and MALDI-TOF MS spectra (right).  
Calculated mass = 2872.39 Da, observed mass = 2870.65 Da.



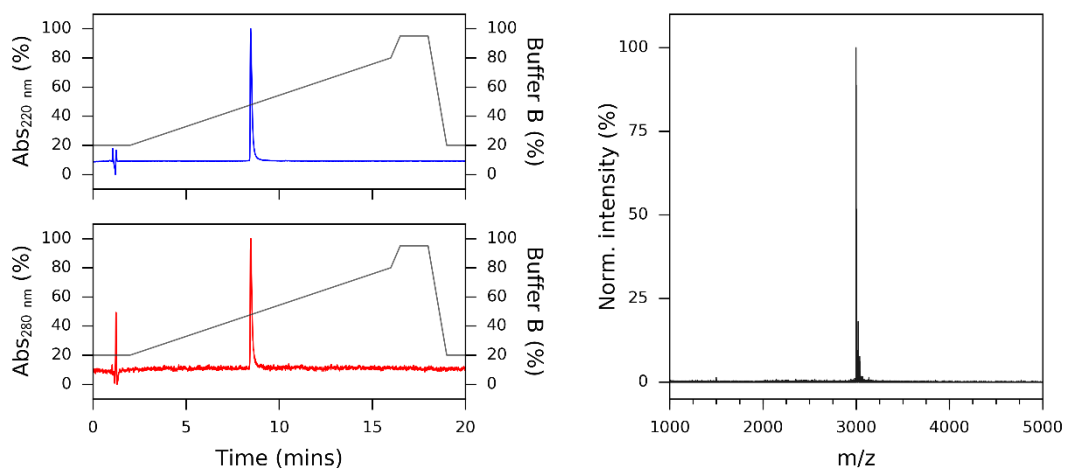


**Figure S2d.** K2-CC-Tri3 HPLC (left; 220 and 280 nm) and MALDI-TOF MS spectra (right). Calculated mass = 3000.56 Da, observed mass = 2998.61 Da.

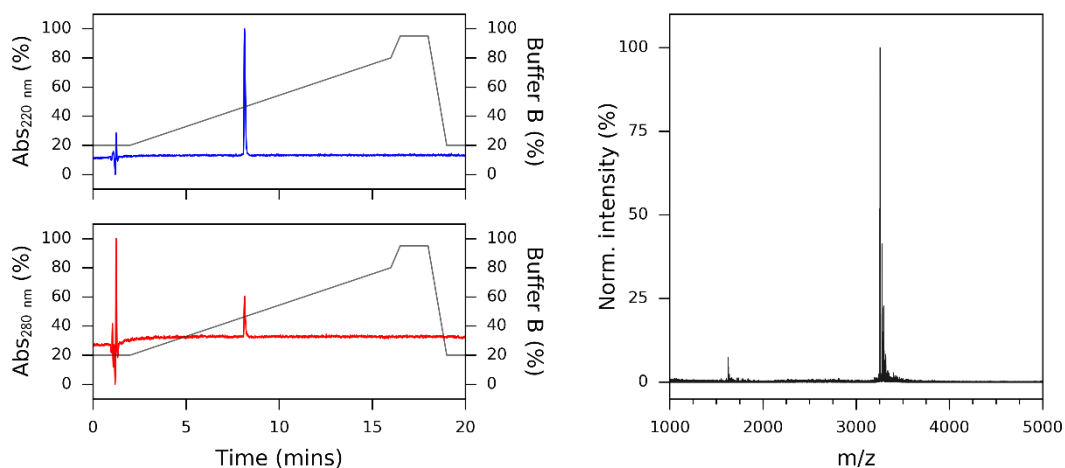


**Figure S2e.** K4-CC-Tri3 HPLC (left; 220 and 280 nm) and MALDI-TOF MS spectra (right). Calculated mass = 3256.95 Da, observed mass = 3255.28 Da.

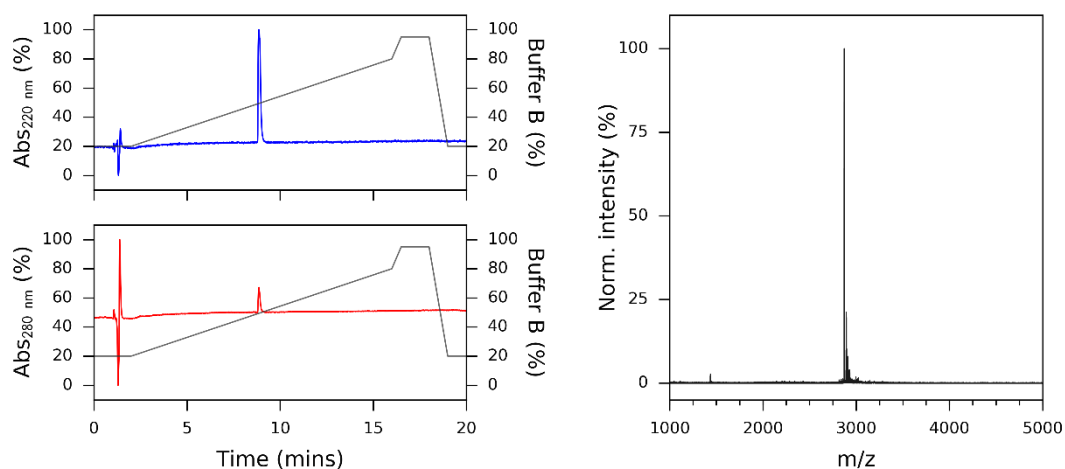


**Figure S2f.** E1-CC-Tri3 HPLC (left; 220 and 280 nm) and MALDI-TOF MS spectra (right). Calculated mass = 2873.33 Da, observed mass = 2871.70 Da.

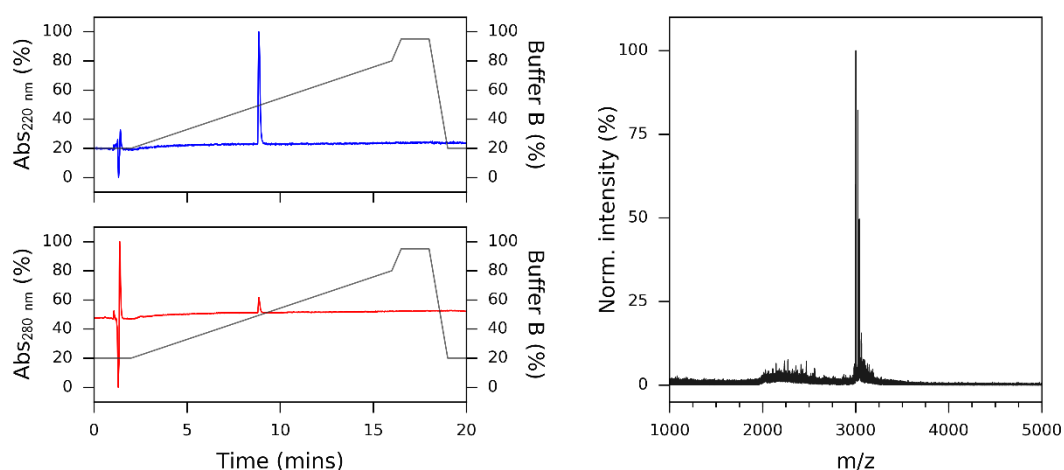


**Figure S2h.** E2-CC-Tri3 HPLC (left; 220 and 280 nm) and MALDI-TOF MS spectra (right). Calculated mass = 3002.44 Da, observed mass = 3001.08 Da.

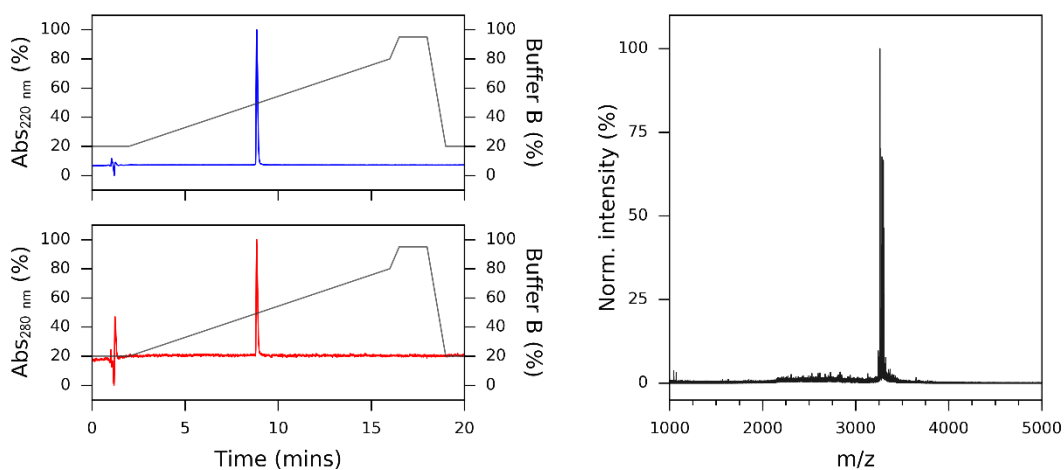


**Figure S2i.** E4-CC-Tri3 HPLC (left; 220 and 280 nm) and MALDI-TOF MS spectra (right). Calculated mass = 3260.71 Da, observed mass = 3260.15 Da.

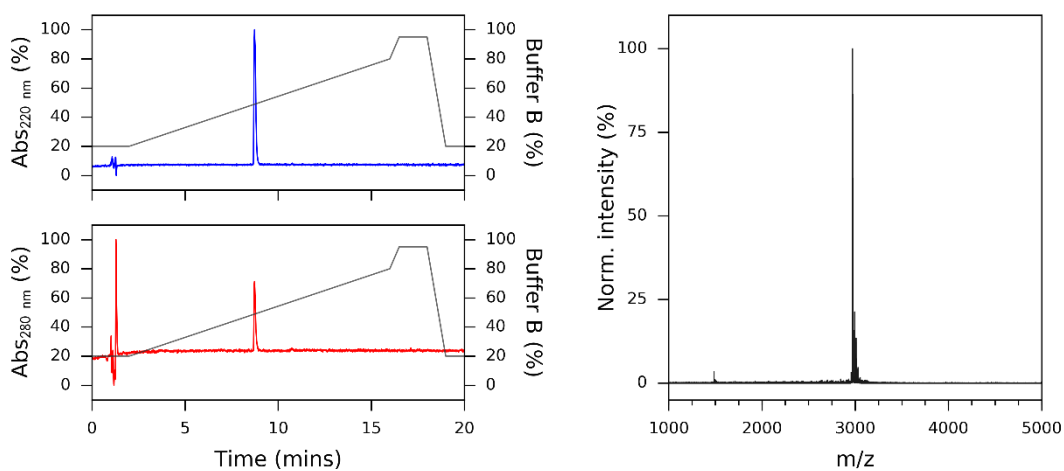


**Figure S2j.** G4-CC-Tri3 HPLC (left; 220 and 280 nm) and MALDI-TOF MS spectra (right). Calculated mass = 2972.46 Da, observed mass = 2971.36 Da.

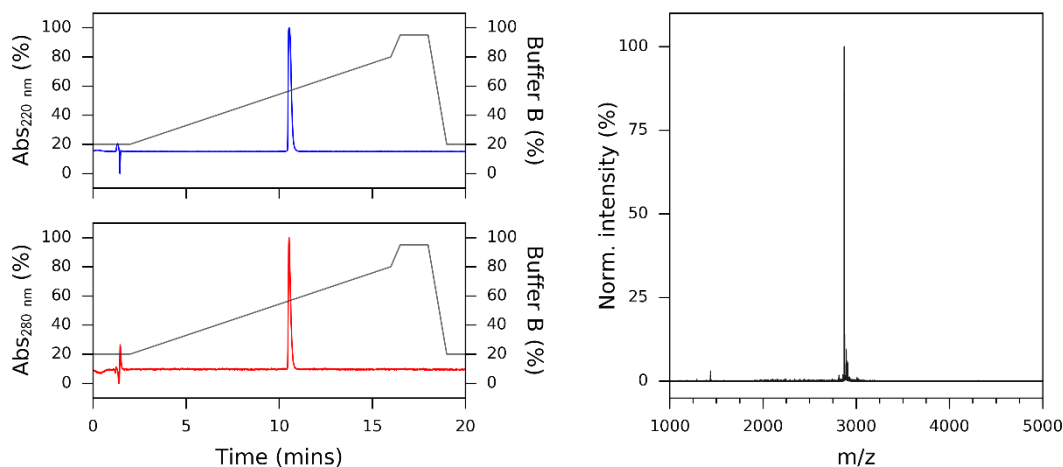


**Figure S2k.** CC-Tri3-K1 HPLC (left; 220 and 280 nm) and MALDI-TOF MS spectra (right).  
Calculated mass = 2872.39 Da, observed mass = 2871.62 Da.

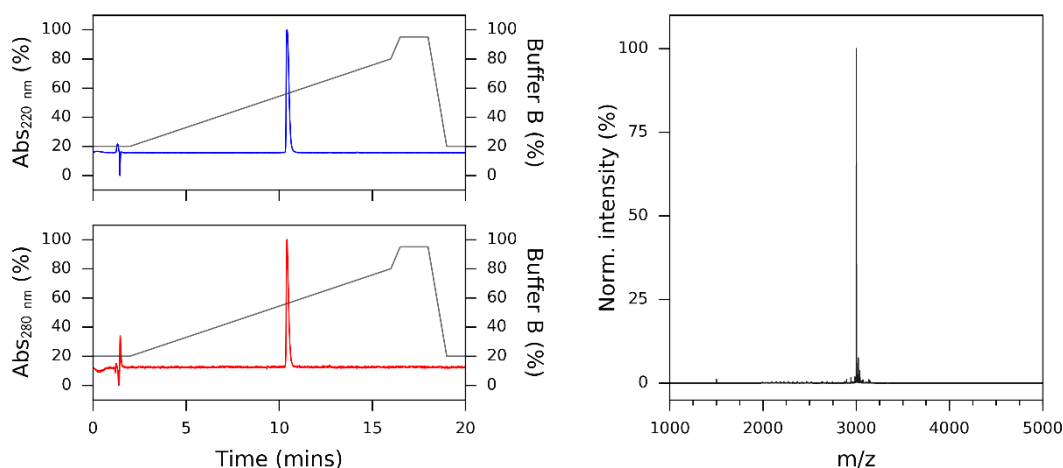


**Figure S2l.** CC-Tri3-K2 HPLC (left; 220 and 280 nm) and MALDI-TOF MS spectra (right).  
Calculated mass = 3000.56 Da, observed mass = 3000.20 Da.

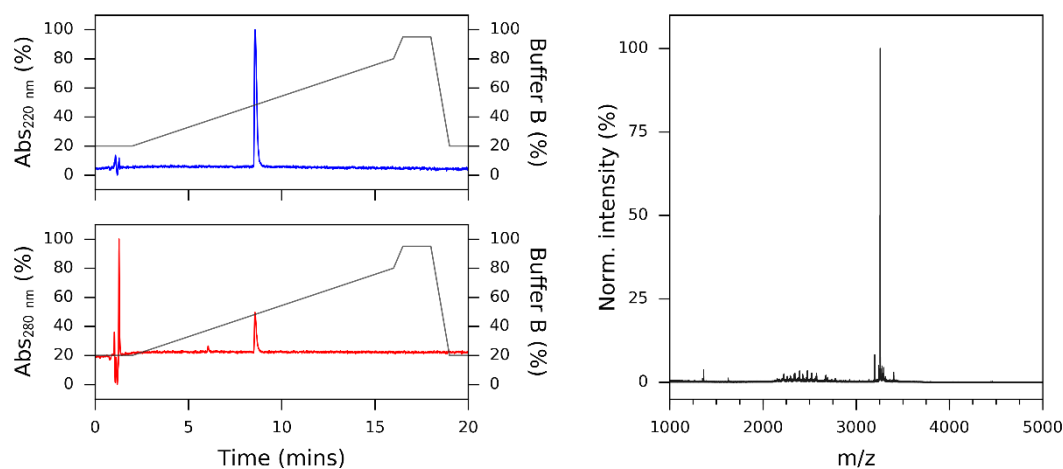


**Figure S2m.** CC-Tri3-K4 HPLC (left; 220 and 280 nm) and MALDI-TOF MS spectra (right).  
Calculated mass = 3256.95 Da, observed mass = 3255.57 Da.

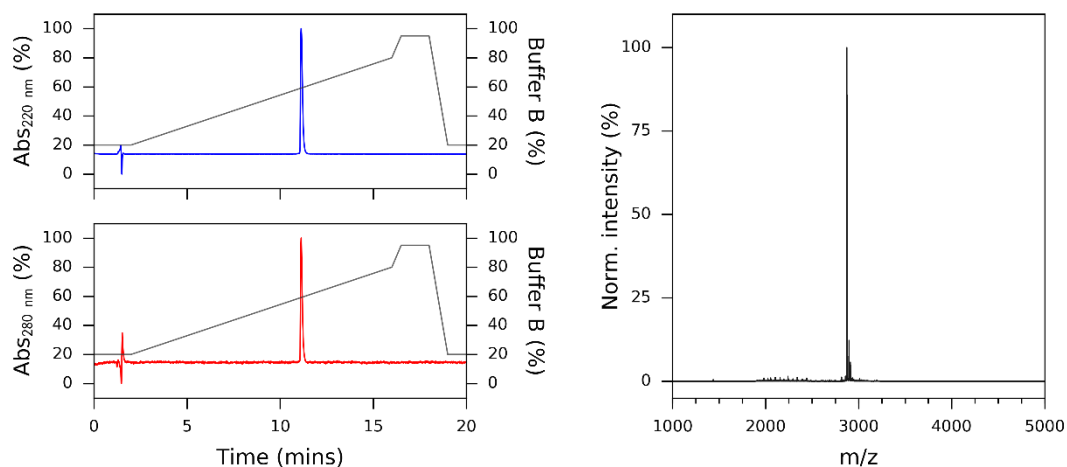


**Figure S2n.** CC-Tri3-E1 HPLC (left; 220 and 280 nm) and MALDI-TOF MS spectra (right). Calculated mass = 2873.33 Da, observed mass = 2873.01 Da.

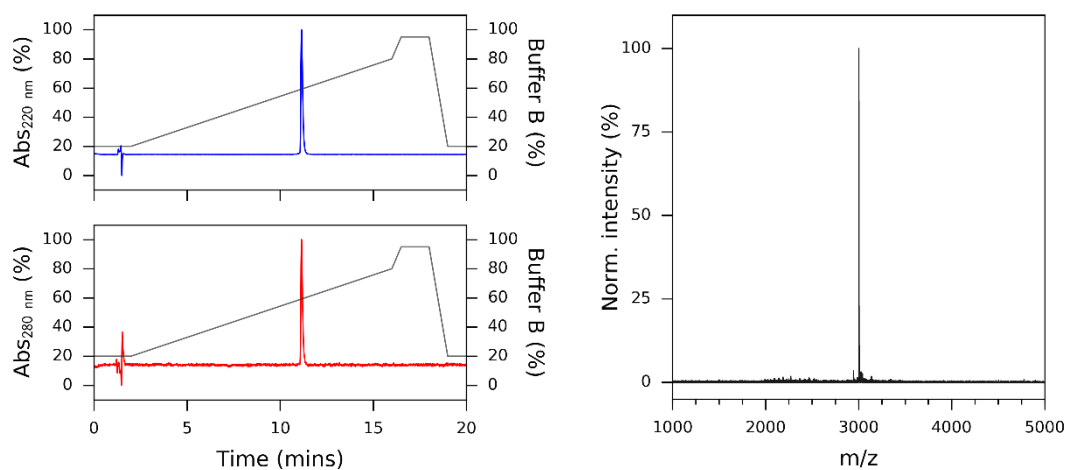


**Figure S2o.** CC-Tri3-E2 HPLC (left; 220 and 280 nm) and MALDI-TOF MS spectra (right). Calculated mass = 3002.44 Da, observed mass = 3002.11 Da.

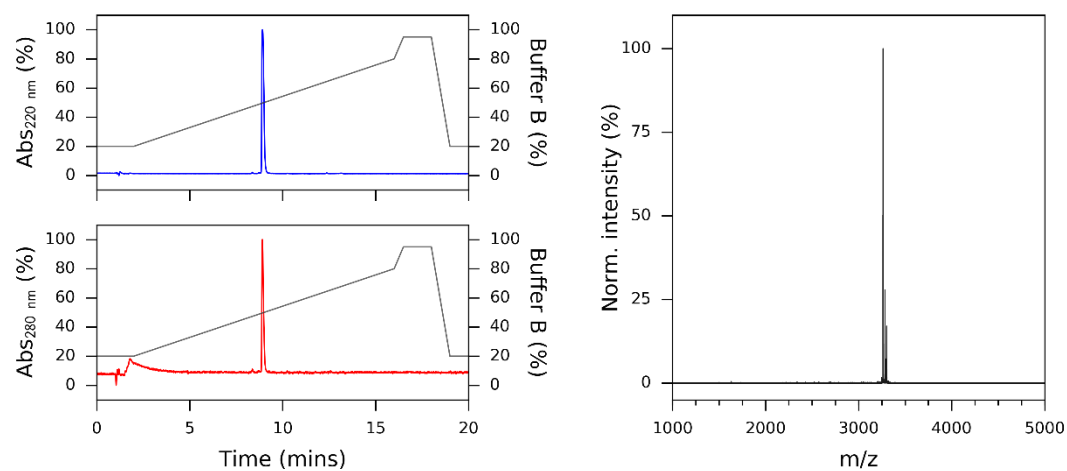


**Figure S2p.** CC-Tri3-E4 HPLC (left; 220 and 280 nm) and MALDI-TOF MS spectra (right). Calculated mass = 3260.71 Da, observed mass = 3261.23 Da.

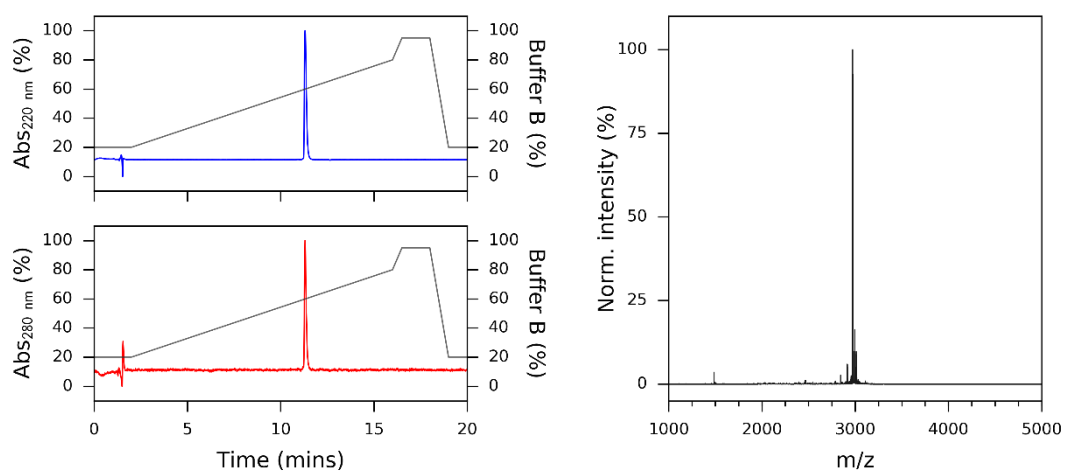


**Figure S2q.** CC-Tri3-G4 HPLC (left; 220 and 280 nm) and MALDI-TOF MS spectra (right).  
 Calculated mass = 2972.46 Da, observed mass = 2971.81 Da.

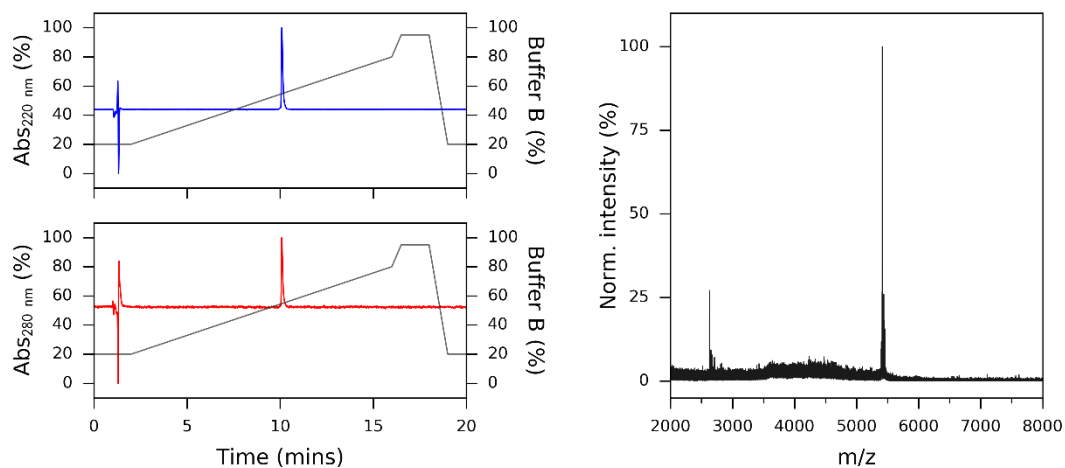


**Figure S3a.** Hub-A HPLC (left; 220 and 280 nm) and MALDI-TOF MS spectra (right). Calculated mass = 5414.24 Da, observed mass = 5412.51 Da.

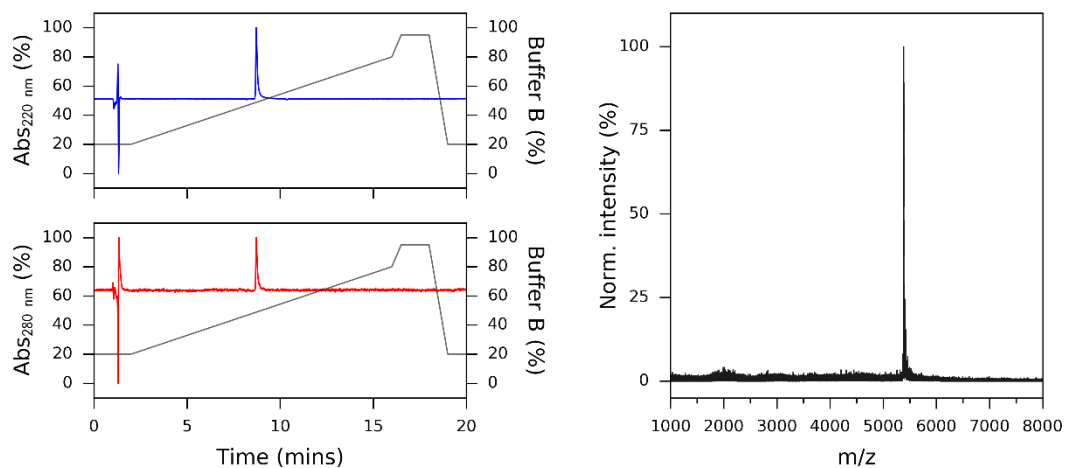


**Figure S3b.** Hub-B HPLC (left; 220 and 280 nm) and MALDI-TOF MS spectra (right). Calculated mass = 3443.92 Da, observed mass = 3444.61 Da.

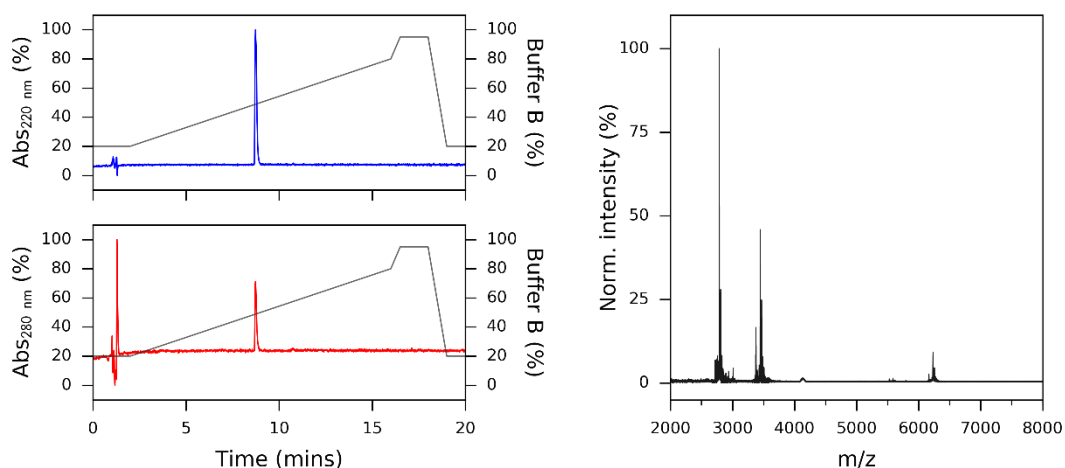


**Figure S3c.** Hub-A<sup>488</sup> HPLC (left; 220 and 280 nm) and MALDI-TOF MS spectra (right). Calculated mass = 6228.01 Da, observed mass = 6227.96 Da.

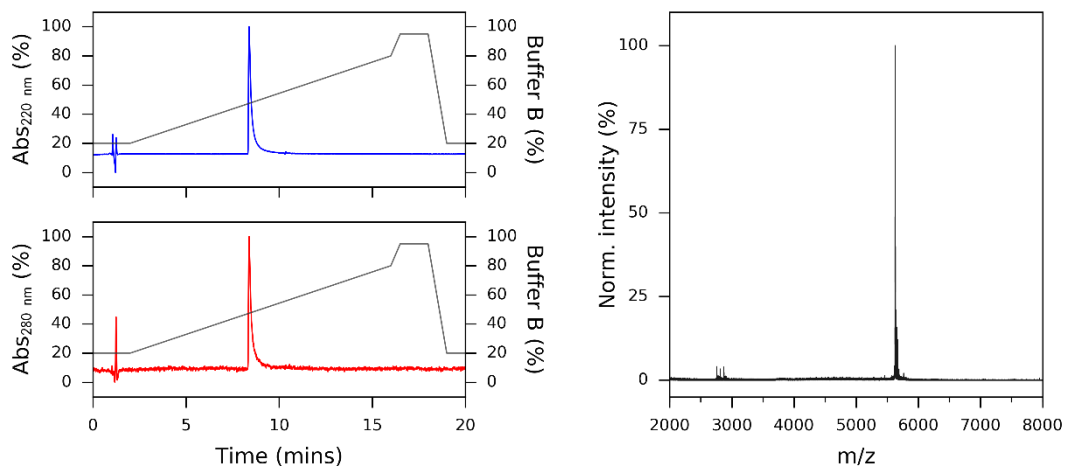


**Figure S3d.** K1-Hub-B HPLC (left; 220 and 280 nm) and MALDI-TOF MS spectra (right).  
Calculated mass = 5627.80 Da, observed mass = 5626.29 Da.

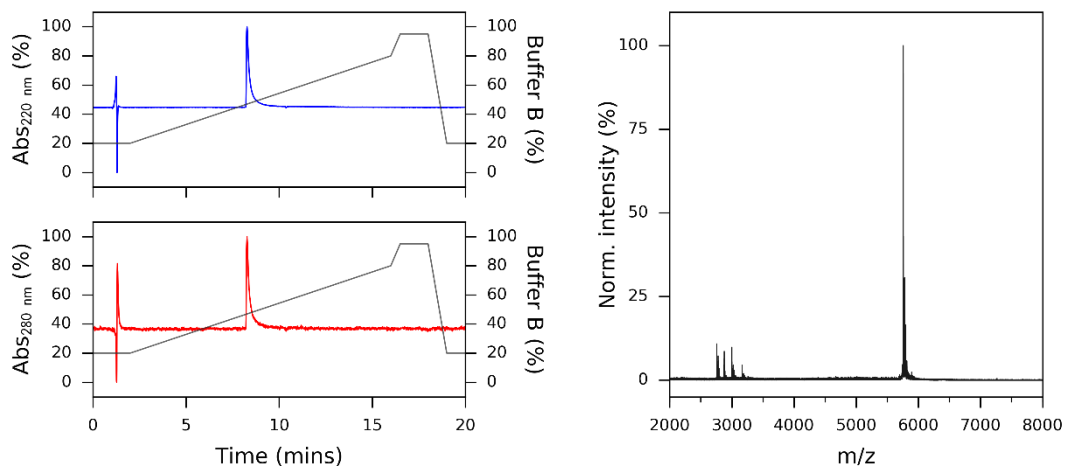


**Figure S3e.** K2-Hub-B HPLC (left; 220 and 280 nm) and MALDI-TOF MS spectra (right).  
Calculated mass = 5755.97 Da, observed mass = 5754.08 Da.

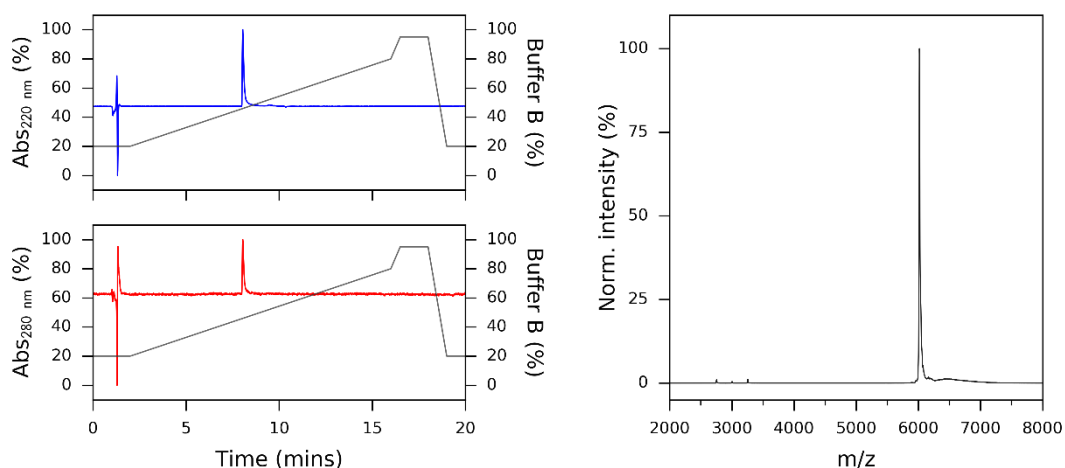


**Figure S3f.** K4-Hub-B HPLC (left; 220 and 280 nm) and MALDI-TOF MS spectra (right).  
Calculated mass = 6012.36 Da, observed mass = 6018.35 Da.

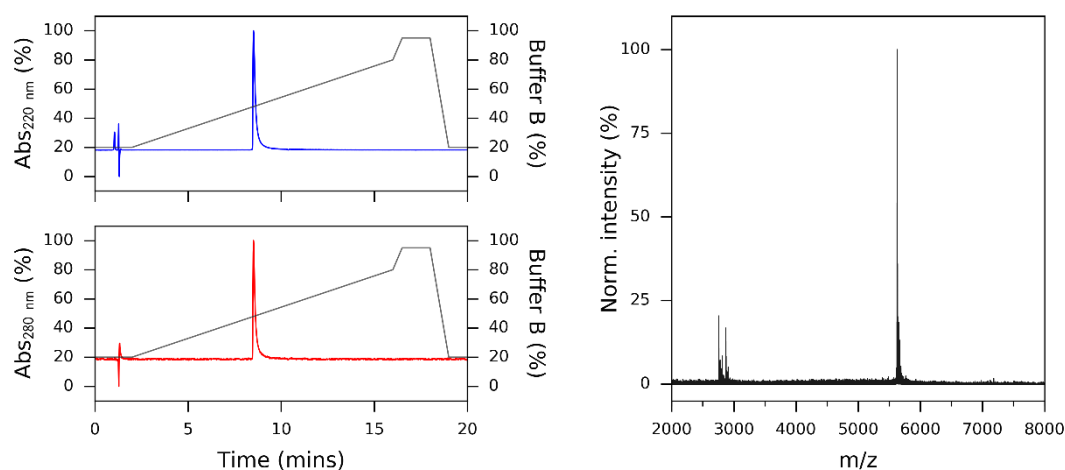


**Figure S3g.** E1-Hub-B HPLC (left; 220 and 280 nm) and MALDI-TOF MS spectra (right). Calculated mass = 5628.74 Da, observed mass = 5626.40 Da.

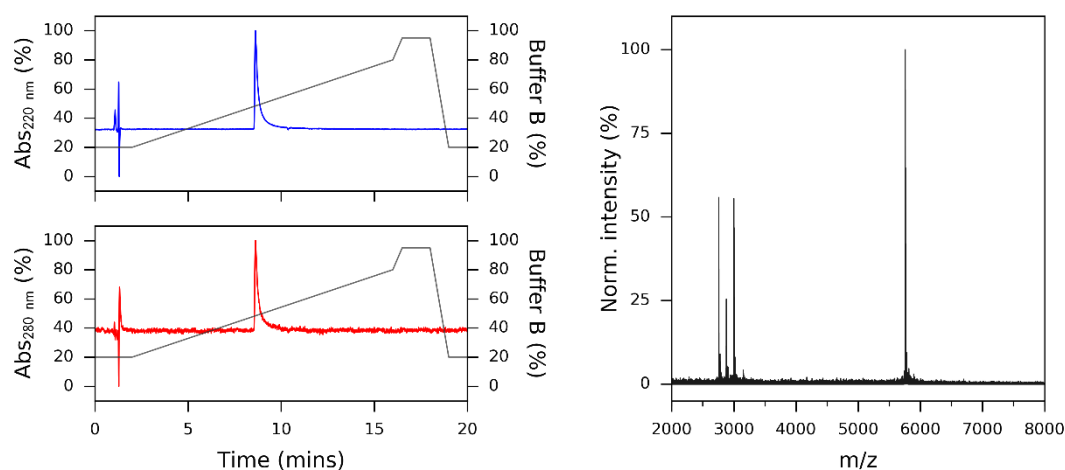


**Figure S3h.** E2-Hub-B HPLC (left; 220 and 280 nm) and MALDI-TOF MS spectra (right). Calculated mass = 5757.85 Da, observed mass = 5755.95 Da.

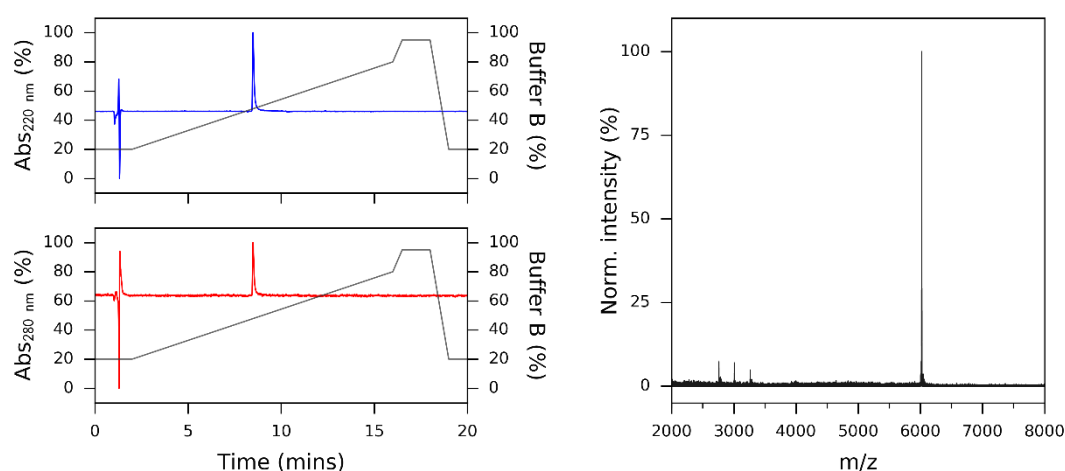


**Figure S3i.** E4-Hub-B HPLC (left; 220 and 280 nm) and MALDI-TOF MS spectra (right). Calculated mass = 6016.12 Da, observed mass = 6018.90 Da.



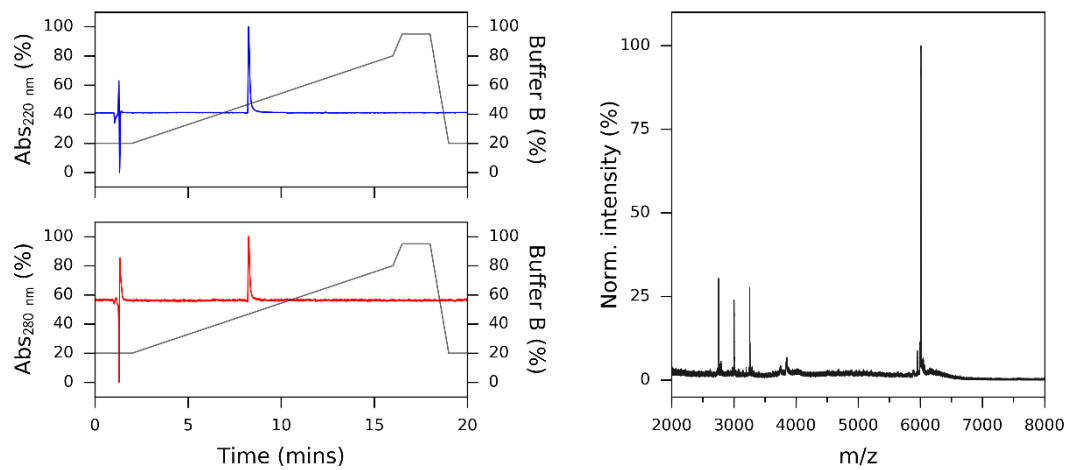


**Figure S3j.** Hub-B-K4 HPLC (left; 220 and 280 nm) and MALDI-TOF MS spectra (right). Calculated mass = 6012.36 Da, observed mass = 6010.63 Da.

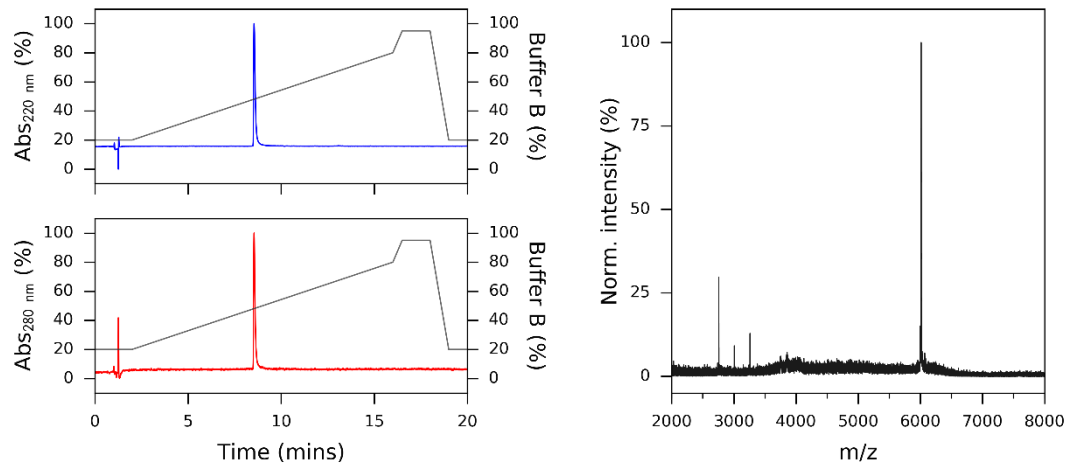


**Figure S3k.** Hub-B-E4 HPLC (left; 220 and 280 nm) and MALDI-TOF MS spectra (right). Calculated mass = 6016.12 Da, observed mass = 6014.59 Da.

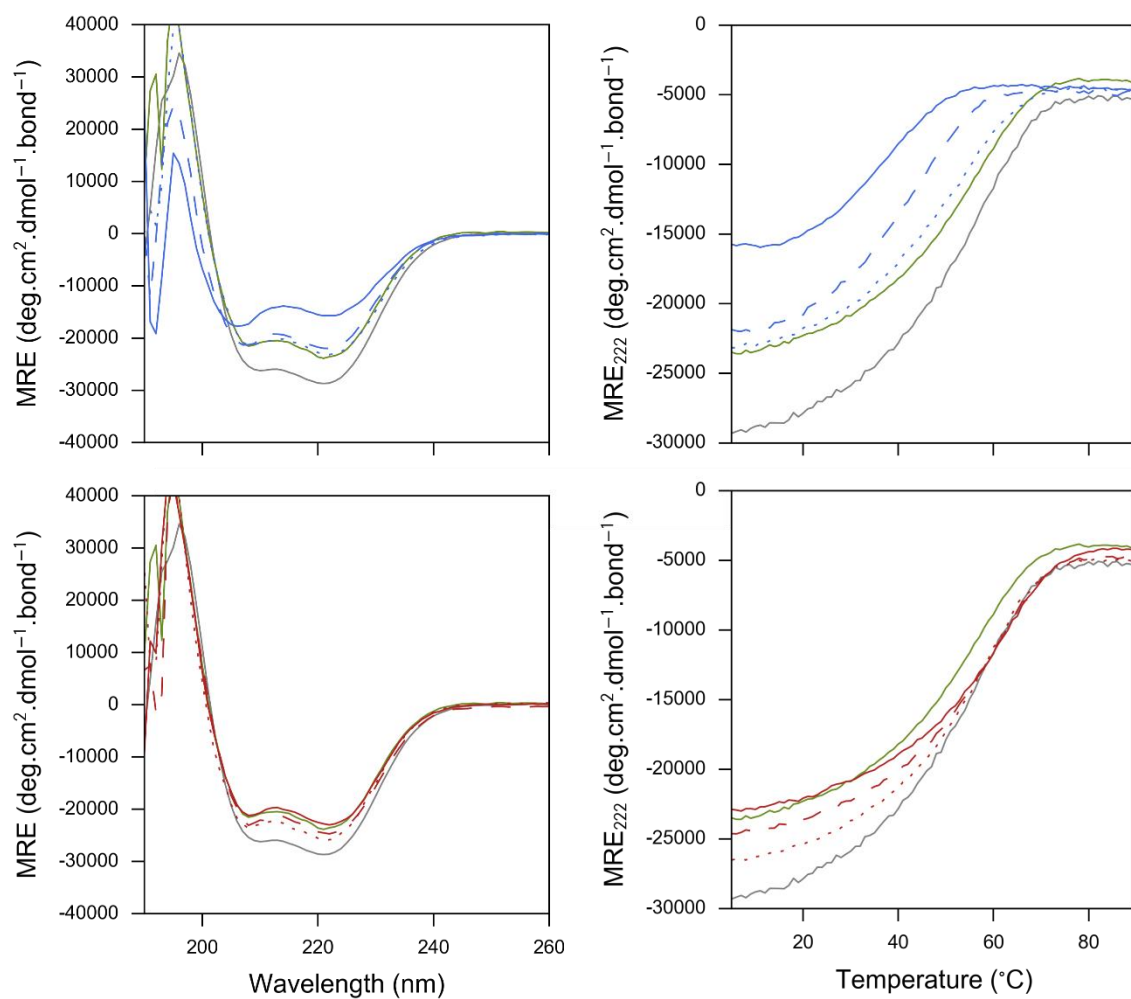


**Figure S4.** Circular dichroism spectra at 5°C (left) and thermal denaturation profiles (right) of CC-Tri3 variants carrying *N*-terminal extensions. CC-Tri3 (grey) and G4-CC-Tri3 (green) are shown alongside K1- (blue; dotted), K2- (blue; dashed) and K4-CC-Tri3 (blue; solid; top panels) or E1- (red; dotted), E2- (red; dashed) and E4-CC-Tri3 (red; solid; bottom panels). Conditions: 50  $\mu$ M peptide, 250  $\mu$ M TCEP, PBS.

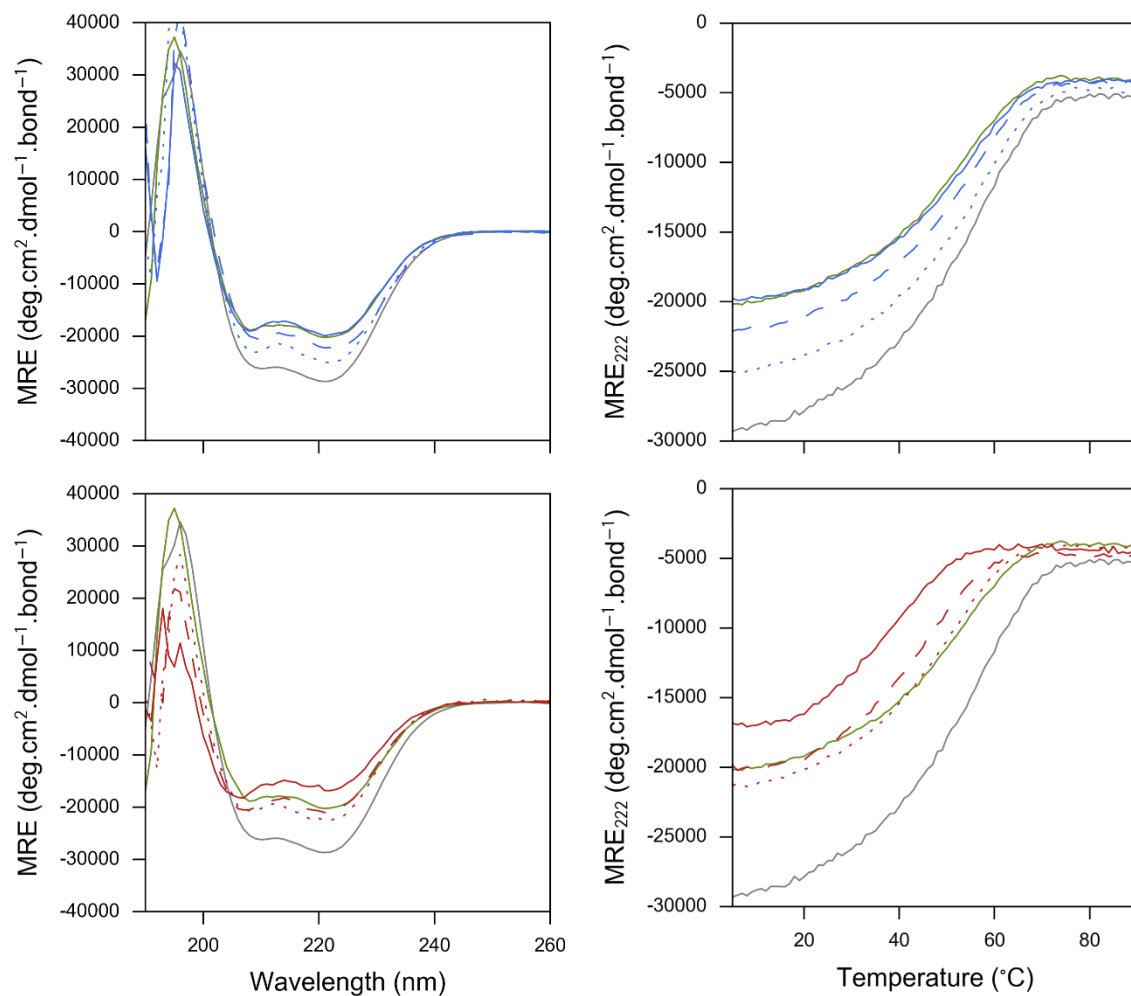


**Figure S5.** Circular dichroism spectra at 5°C (left) and thermal denaturation profiles (right) of CC-Tri3 variants carrying C-terminal extensions. CC-Tri3 (grey) and CC-Tri3-G4 (green) are shown alongside CC-Tri3-K1 (blue; dotted), -K2 (blue; dashed) and -K4 (blue; solid; top panels) or CC-Tri3-E1 (red; dotted), -E2 (red; dashed) and -E4 (red; solid; bottom panels). Conditions: 50  $\mu$ M peptide, 250  $\mu$ M TCEP, PBS.

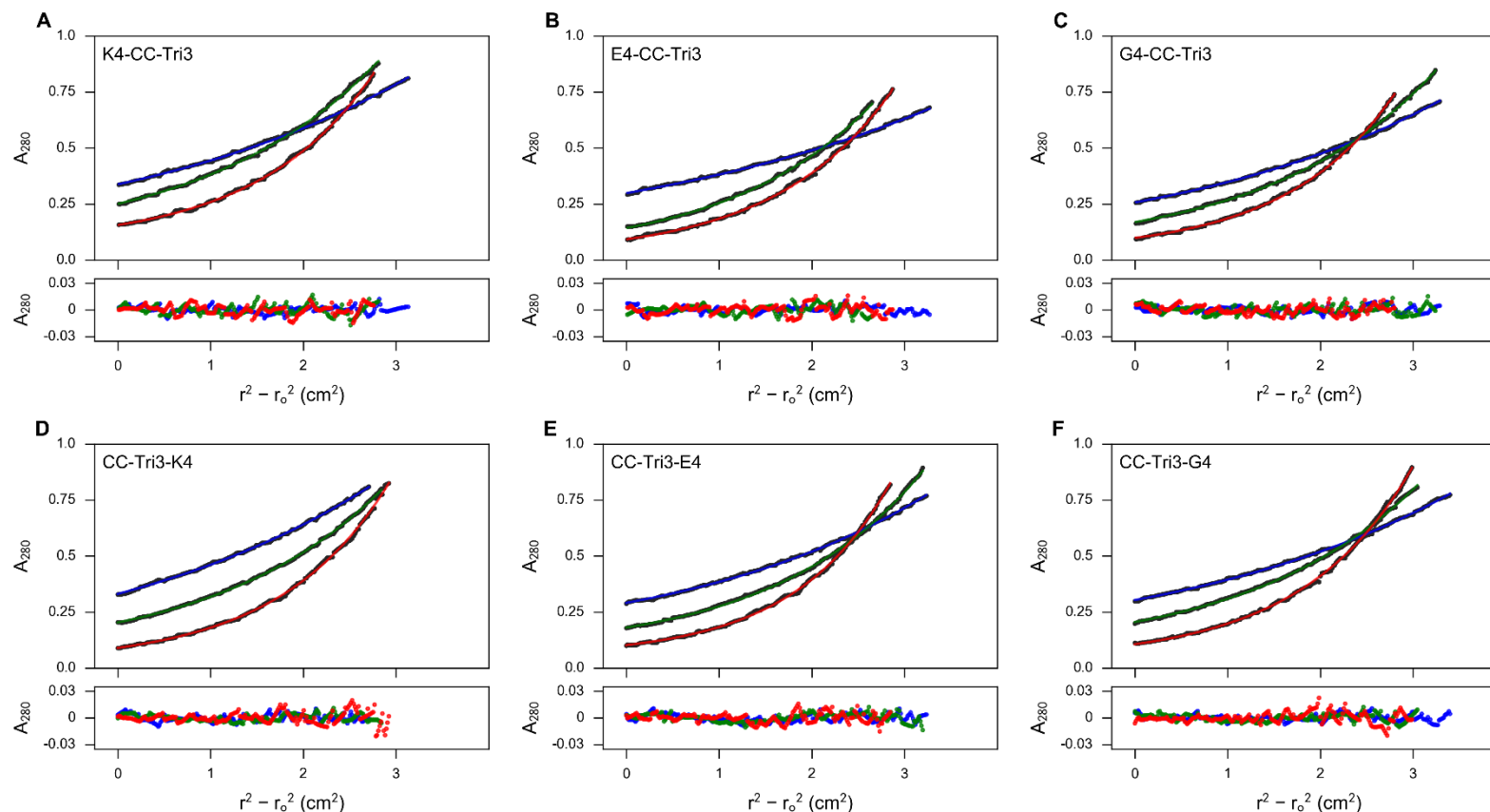


**Figure S6.** Sedimentation equilibrium analytical ultracentrifugation data (top panels; dots), fitted single-ideal species model curves (top panels; black lines) at 26 (blue), 34 (green) and 42 (red) krpm and residuals (bottom panels; same colour scheme). Conditions: 325  $\mu$ M peptide, 1.63 mM TCEP, PBS. **A** K4-CC-Tri3. Fitted mass of 8521 Da (2.8 x monomer mass, 95 % confidence limits 8908 – 9012 Da). **B** E4-CC-Tri3. Fitted mass of 9782 Da (3.0 x monomer mass, 95 % confidence limits 9744 – 9819 Da). **C** G4-CC-Tri3. Fitted mass of 8860 Da (3.0 x monomer mass, 95 % confidence limits 8828 – 8892 Da). **D** CC-Tri3-K4. Fitted mass of 9484 Da (2.9 x monomer mass, 95 % confidence limits 9429 – 9540 Da). **E** CC-Tri3-E4. Fitted mass of 9697 Da (3.0 x monomer mass, 95 % confidence limits 9656 – 9739 Da). **F** CC-Tri3-G4. Fitted mass of 8665 Da (2.9 x monomer mass, 95 % confidence limits 8625 – 8706 Da).

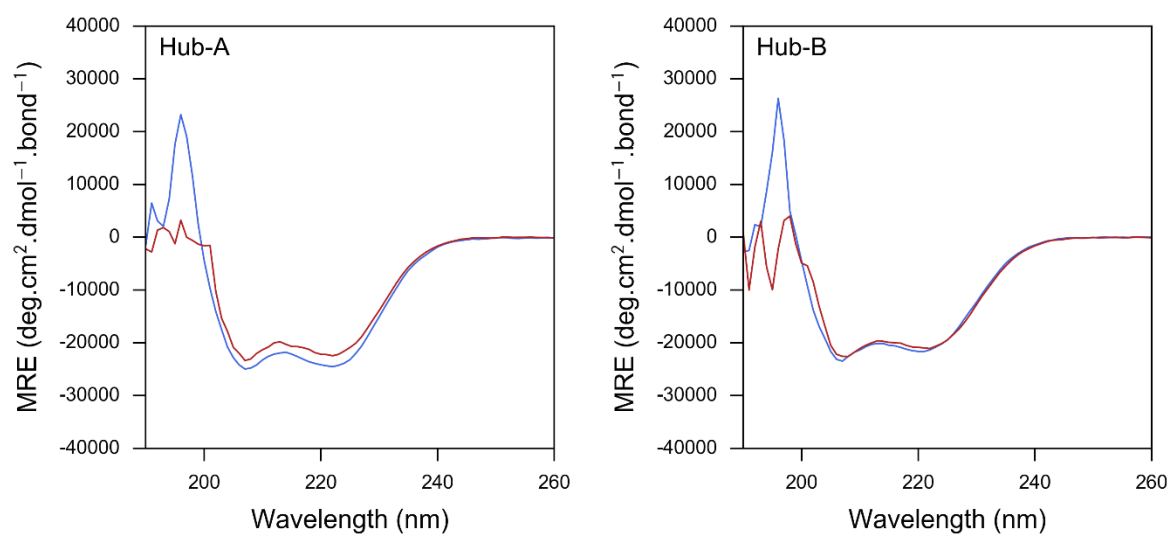


**Figure S7.** Circular dichroism spectra of Hub-A (left) and Hub-B (right) at 50  $\mu\text{M}$  in PBS (blue) and HBS (red; 25 mM HEPES, 150 mM NaCl, pH 7).

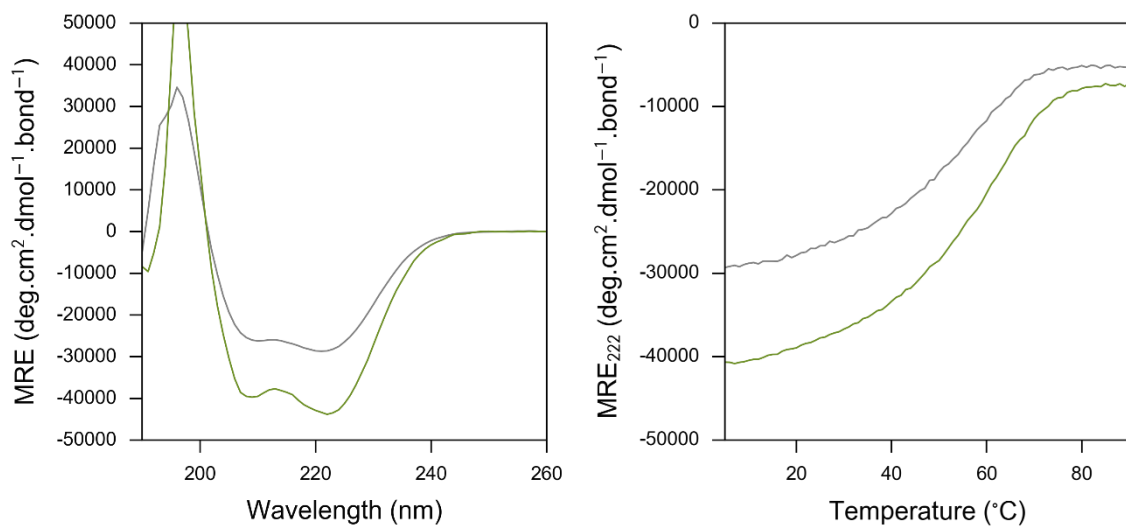


**Figure S8.** Circular dichroism spectra at 5°C (left) and thermal denaturation profiles (right) of CC-Tri3 (grey;  $T_M = 56$  °C) and CC-Tri3<sup>488</sup> (green;  $T_M = 61$  °C). Conditions: 50  $\mu$ M peptide, 250  $\mu$ M TCEP, PBS.

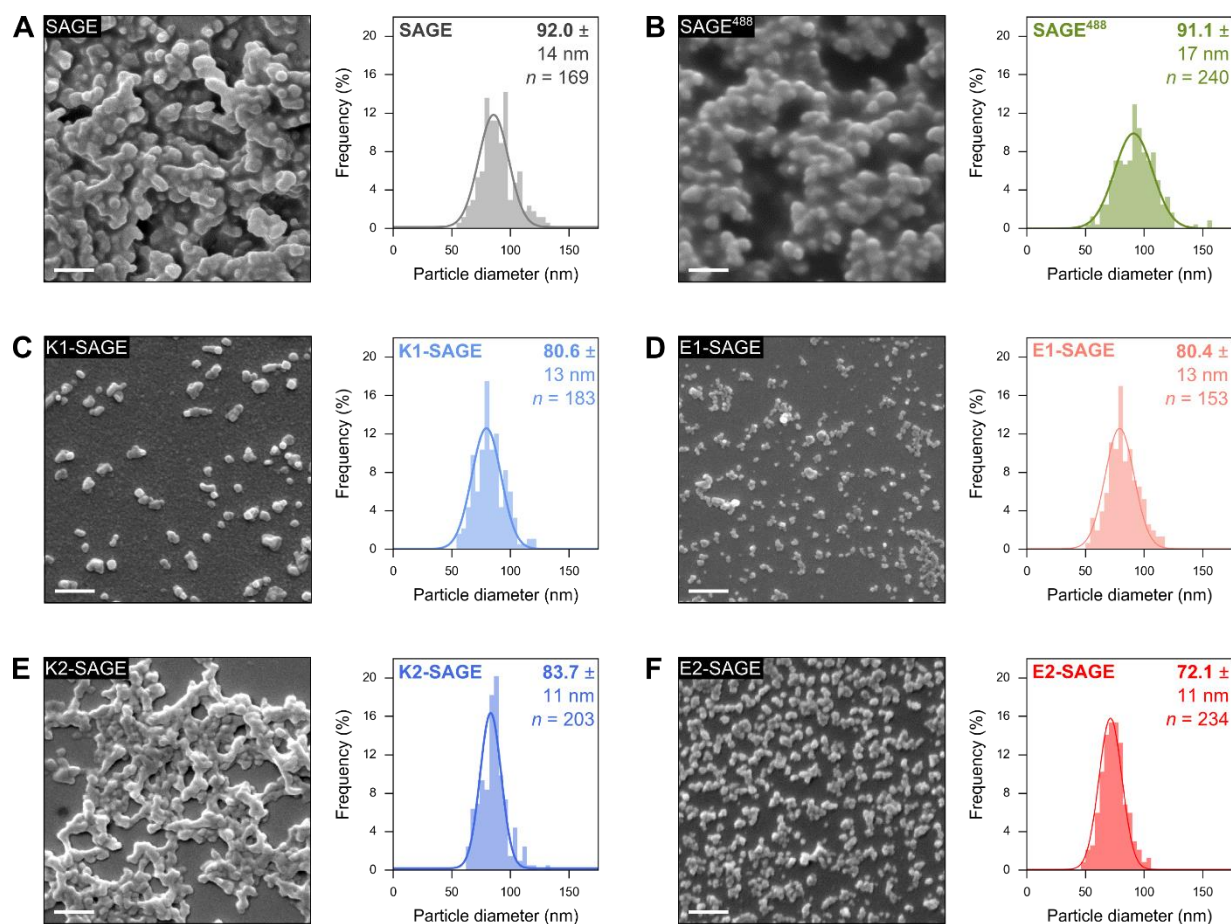


**Figure S9.** Scanning electron microscopy analysis of SAGE (A), SAGE<sup>488</sup> (B), K1-SAGE (C), E1-SAGE (D), K2-SAGE (E) and E2-SAGE (F). Representative micrographs (left, scale bars: 500 nm) are displayed alongside diameter quantification and Gaussian fits across multiple micrographs (right, diameters shown as mean  $\pm$  standard deviation). SAGEs formed at 50  $\mu$ M peptide concentration for 1 h at RT in HBS.

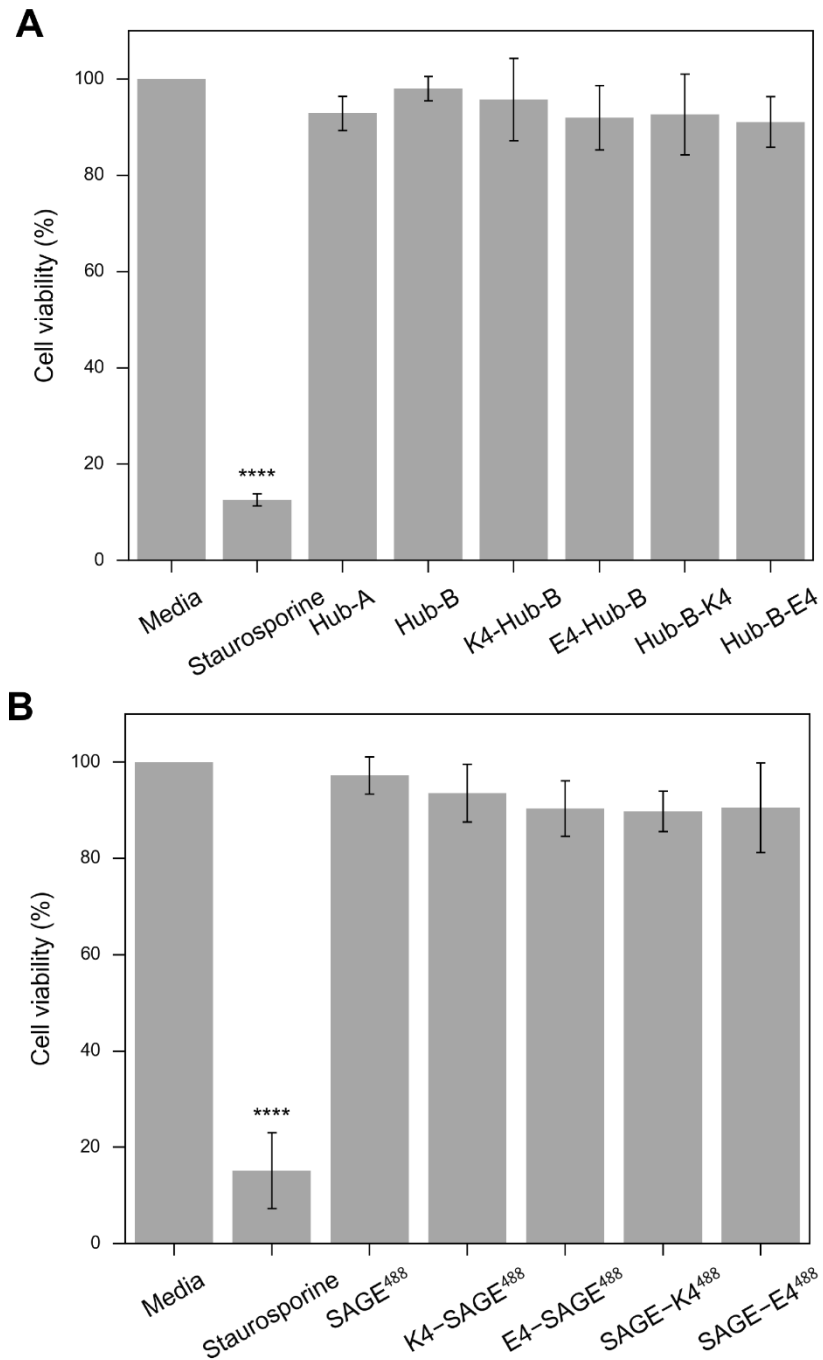


**Figure S10.** Cytotoxicity of SAGE components (**A**) and assembled particles (**B**) at 10  $\mu$ M peptide concentration to HeLa cells after 24 h. Media and 1  $\mu$ M staurosporine were used as negative and positive controls, respectively. Cell viability was calculated using the XTT assay and normalised to Media control. One-way ANOVA with a Dunnett's multiple comparisons test was used to calculate *p*-values (\*\*\*\* indicates *p*-value < 0.0001).



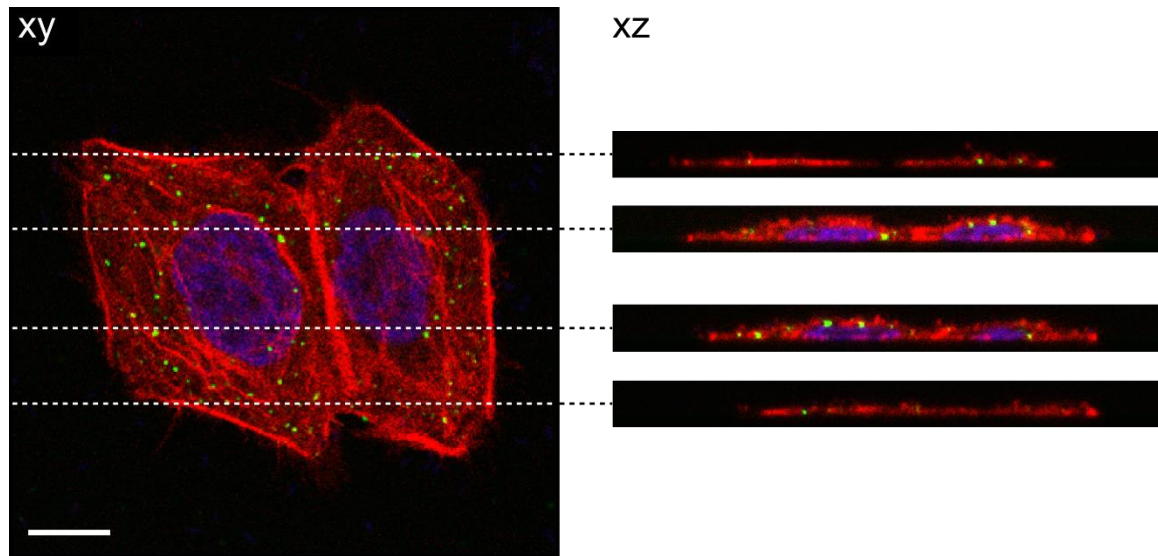


**Figure S11.** Confocal sections extracted from z stacks of HeLa cells after 2 h exposure to SAGE<sup>488</sup>. Dotted lines indicate the y coordinate of each xz section. SAGE particles are colored green and cells were labelled for F-actin (red; Alexa Fluor 594 Phalloidin) and nuclei (blue; DAPI). Scale bar: 10  $\mu\text{m}$ .

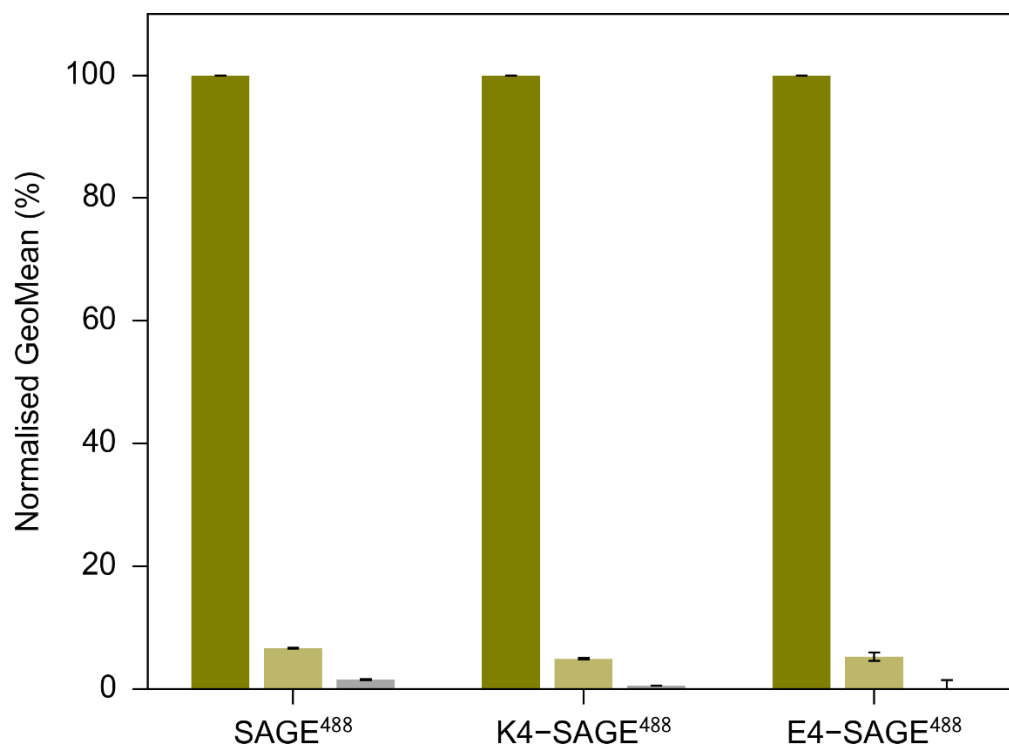


**Figure S12.** Flow cytometry analysis of SAGE<sup>488</sup>, K4-SAGE<sup>488</sup> and E4-SAGE<sup>488</sup> internalization after 2 h incubation at 37 °C (green), 20 °C (khaki) and 4 °C (grey). Cell population GeoMean is normalised to the 37 °C data for each SAGE composition. Bar heights show statistical mean  $\pm$  standard deviation ( $n = 3$ ).

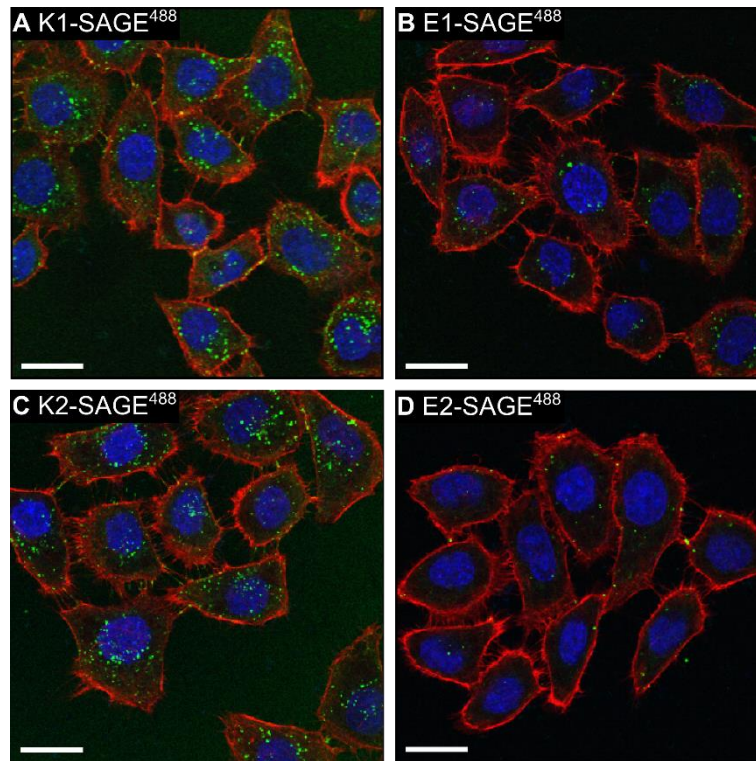


**Figure S13.** Representative confocal microscopy images of HeLa cells after 2 h exposure to K1-SAGE<sup>488</sup> (A; green), E1-SAGE<sup>488</sup> (B), K2-SAGE<sup>488</sup> (C) or E2-SAGE<sup>488</sup> (D). SAGE particles are colored green and cells were labeled for F-actin (red) and nuclei (blue). Scale bars: 10 μm.

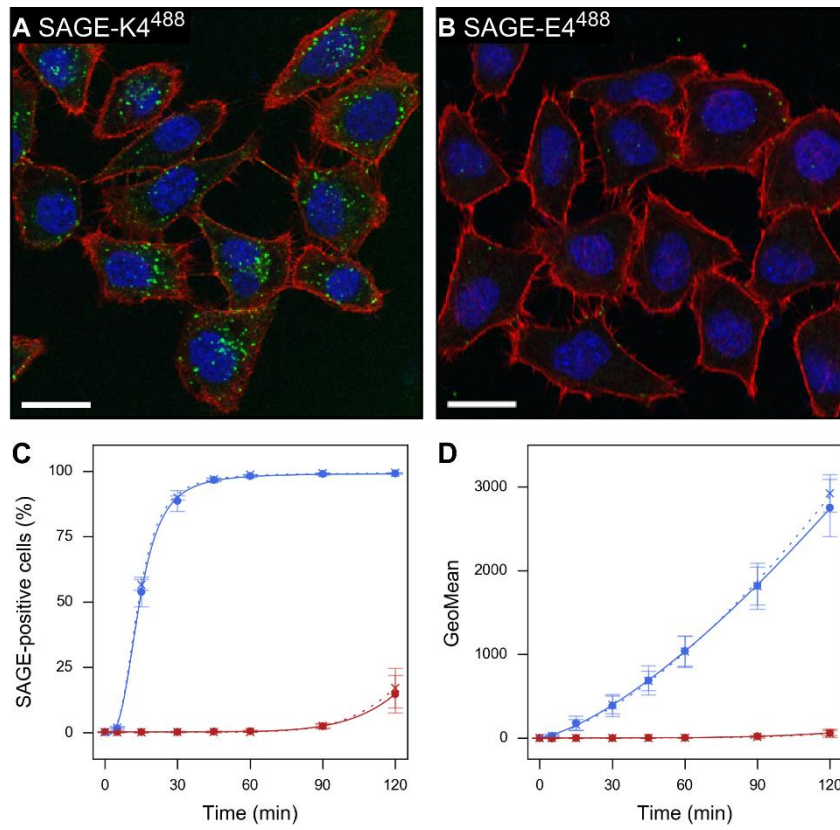


**Figure S14.** Representative confocal microscopy images of HeLa cells after 2 h exposure to SAGE-K4<sup>488</sup> (A) or SAGE-E4<sup>488</sup> (B). SAGE particles are colored green and cells were labeled for F-actin (red) and nuclei (blue). Scale bars: 10 μm. Flow cytometry analysis of SAGE-K4<sup>488</sup> (blue; dashed, crosses) and SAGE-E4<sup>488</sup> (red; dashed, crosses) internalization shown as rate at which cells become SAGE positive (C) and total intracellular load (D) compared to K4-SAGE<sup>488</sup> (blue; solid, circles) and E4-SAGE<sup>488</sup> (red; solid, circles). Points show statistical mean ± standard deviation (n = 3).

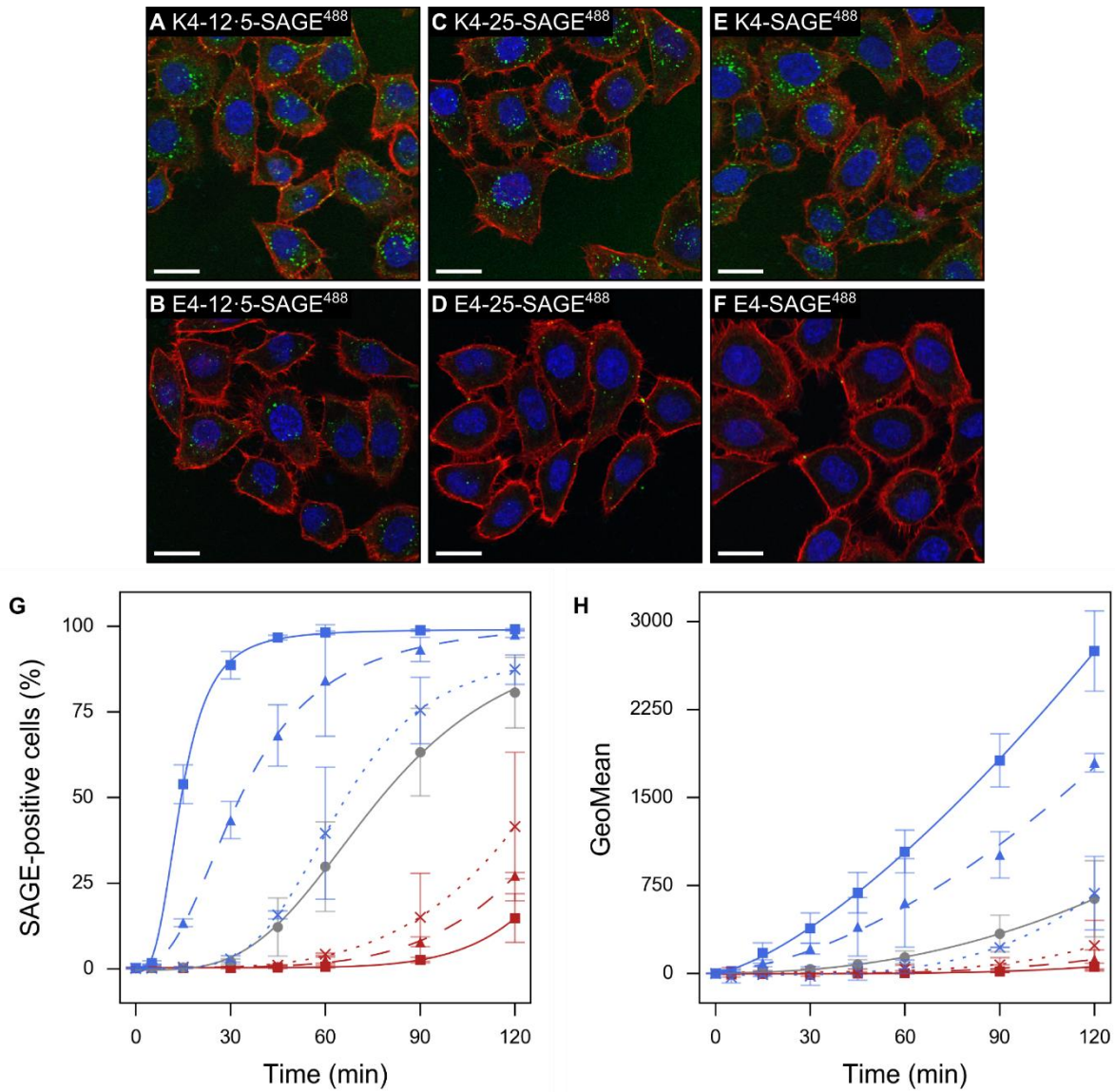


**Figure S15.** Representative confocal microscopy images of HeLa cells after 2 h exposure to K4-12-5-SAGE<sup>488</sup> (A), E4-12-5-SAGE<sup>488</sup> (B), K4-25-SAGE<sup>488</sup> (C), E4-25-SAGE<sup>488</sup> (D), K4-SAGE<sup>488</sup> (E) or E4-SAGE<sup>488</sup> (F) (green). SAGE particles are colored green and cells were labeled for F-actin (red) and nuclei (blue). Scale bars: 10 μm. Flow cytometry analysis of SAGE<sup>488</sup> (grey), K4-12-5-SAGE<sup>488</sup> (blue; dotted, crosses), K4-25-SAGE<sup>488</sup> (blue; dashed, triangles), K4-SAGE<sup>488</sup> (blue; solid, squares) E4-12-5-SAGE<sup>488</sup> (red; dotted, crosses), E4-25-SAGE<sup>488</sup> (red; dashed, triangles), and E4-SAGE<sup>488</sup> (red; solid, squares) internalisation by HeLa cells represented as the percentage of cells deemed SAGE positive (G) and population GeoMean (H). Points show statistical mean ± standard deviation ( $n = 3$ ).

Peptide	Sequence <i>gabcdef gabcdef gabcdef</i>	FH (%)	T <sub>M</sub> (°C)
CC-Tri3	Ac- G EIAAIKK EIAAIKC EIAAIKQ GYG -NH <sub>2</sub>	79 ± 1.1	56 ± 1.2
CC-Di-A	Ac- G EIAALEK ENAALEC EIAALEQ GWW -NH <sub>2</sub>	-	-
CC-Di-B	Ac- G KIAALKK KNAALKC KIAALKQ GYW -NH <sub>2</sub>	-	-
CC-Tri3 <sup>488</sup>	Ac- G EIAAIKK EIAAIKC EIAAIKQ GYG GGK(*) G-NH <sub>2</sub>	-	-
K1-CC-Tri3	Ac- K GG G EIAAIKK EIAAIKC EIAAIKQ GYG -NH <sub>2</sub>	59 ± 3.7	51 ± 1.9
K2-CC-Tri3	Ac- KK GG G EIAAIKK EIAAIKC EIAAIKQ GYG -NH <sub>2</sub>	51 ± 6.0	44 ± 0.42
K4-CC-Tri3	Ac-KKKK GG G EIAAIKK EIAAIKC EIAAIKQ GYG -NH <sub>2</sub>	39 ± 2.2	37 ± 1.2
E1-CC-Tri3	Ac- E GG G EIAAIKK EIAAIKC EIAAIKQ GYG -NH <sub>2</sub>	68 ± 1.8	59 ± 0.92
E2-CC-Tri3	Ac- EE GG G EIAAIKK EIAAIKC EIAAIKQ GYG -NH <sub>2</sub>	63 ± 2.0	60 ± 0.53
E4-CC-Tri3	Ac-EEEE GG G EIAAIKK EIAAIKC EIAAIKQ GYG -NH <sub>2</sub>	59 ± 1.1	61 ± 0.42
G4-CC-Tri3	Ac-GGGG GG G EIAAIKK EIAAIKC EIAAIKQ GYG -NH <sub>2</sub>	56 ± 4.6	55 ± 0.49
CC-Tri3-K1	Ac- G EIAAIKK EIAAIKC EIAAIKQ GYG GG K -NH <sub>2</sub>	65 ± 2.9	56 ± 1.2
CC-Tri3-K2	Ac- G EIAAIKK EIAAIKC EIAAIKQ GYG GG KK -NH <sub>2</sub>	56 ± 2.5	56 ± 0.70
CC-Tri3-K4	Ac- G EIAAIKK EIAAIKC EIAAIKQ GYG GG KKKK-NH <sub>2</sub>	51 ± 0.61	55 ± 0.47
CC-Tri3-E1	Ac- G EIAAIKK EIAAIKC EIAAIKQ GYG GG E -NH <sub>2</sub>	56 ± 3.4	50 ± 1.2
CC-Tri3-E2	Ac- G EIAAIKK EIAAIKC EIAAIKQ GYG GG EE -NH <sub>2</sub>	54 ± 1.7	45 ± 0.46
CC-Tri3-E4	Ac- G EIAAIKK EIAAIKC EIAAIKQ GYG GG EEEE-NH <sub>2</sub>	39 ± 4.9	39 ± 0.99
CC-Tri3-G4	Ac- G EIAAIKK EIAAIKC EIAAIKQ GYG GG GGGG-NH <sub>2</sub>	52 ± 0.76	54 ± 0.47

**Table S1.** Sequences and circular dichroism summary of all synthetic peptides discussed in this study. Peptide sequences are displayed below heptad repeat. K(\*) denotes coupling of Alexa Fluor 488 to the side chain of a Lys residue. Circular dichroism spectra were recorded at 50 µM peptide concentration in PBS. Fraction helix (FH) and T<sub>M</sub> values were calculated as described in the Methods and represent mean ± standard deviation, *n* = 3. Only data collected in triplicate are displayed.

Hub peptide	Homotrimer component	Heterodimer component
Hub-A	CC-Tri3	CC-Di-A
Hub-B	CC-Tri3	CC-Di-B
Hub-A <sup>488</sup>	CC-Tri3 <sup>488</sup>	CC-Di-A
K1-Hub-B	K1-CC-Tri3	CC-Di-B
K2-Hub-B	K2-CC-Tri3	CC-Di-B
K4-Hub-B	K4-CC-Tri3	CC-Di-B
E1-Hub-B	E1-CC-Tri3	CC-Di-B
E2-Hub-B	E2-CC-Tri3	CC-Di-B
E4-Hub-B	E4-CC-Tri3	CC-Di-B
Hub-B-K4	CC-Tri3-K4	CC-Di-B
Hub-B-E4	CC-Tri3-E4	CC-Di-B

**Table S2.** The component peptides of all hub peptides discussed in this study.

Name	Hub-A components	Hub-B components	Relative surface charge	Pictogram
SAGE	50 % Hub-A	50 % Hub-B	0	
SAGE <sup>488</sup>	45 % Hub-A : 5 % Hub-A <sup>488</sup>	50 % Hub-B	0	
K1-SAGE	50 % Hub-A	50 % K1-Hub-B	+1	
K2-SAGE	50 % Hub-A	50 % K2-Hub-B	+2	
K4-SAGE	50 % Hub-A	50 % K4-Hub-B	+4	
E1-SAGE	50 % Hub-A	50 % E1-Hub-B	-1	
E2-SAGE	50 % Hub-A	50 % E2-Hub-B	-2	
E4-SAGE	50 % Hub-A	50 % E4-Hub-B	-4	
K1-SAGE <sup>488</sup>	45 % Hub-A : 5 % Hub-A <sup>488</sup>	50 % K1-Hub-B	+1	
K2-SAGE <sup>488</sup>	45 % Hub-A : 5 % Hub-A <sup>488</sup>	50 % K2-Hub-B	+2	
K4-SAGE <sup>488</sup>	45 % Hub-A : 5 % Hub-A <sup>488</sup>	50 % K4-Hub-B	+4	
E1-SAGE <sup>488</sup>	45 % Hub-A : 5 % Hub-A <sup>488</sup>	50 % E1-Hub-B	-1	
E2-SAGE <sup>488</sup>	45 % Hub-A : 5 % Hub-A <sup>488</sup>	50 % E2-Hub-B	-2	
E4-SAGE <sup>488</sup>	45 % Hub-A : 5 % Hub-A <sup>488</sup>	50 % E4-Hub-B	-4	
SAGE-K4 <sup>488</sup>	45 % Hub-A : 5 % Hub-A <sup>488</sup>	50 % Hub-B-K4	0	
SAGE-E4 <sup>488</sup>	45 % Hub-A : 5 % Hub-A <sup>488</sup>	50 % Hub-B-E4	0	
K4-12.5-SAGE <sup>488</sup>	45 % Hub-A : 5 % Hub-A <sup>488</sup>	37.5 % Hub-B : 12.5 % K4-Hub-B	+1	
K4-25-SAGE <sup>488</sup>	45 % Hub-A : 5 % Hub-A <sup>488</sup>	25 % Hub-B : 25 % K4-Hub-B	+2	
E4-12.5-SAGE <sup>488</sup>	45 % Hub-A : 5 % Hub-A <sup>488</sup>	37.5 % Hub-B : 12.5 % E4-Hub-B	-1	
E4-25-SAGE <sup>488</sup>	45 % Hub-A : 5 % Hub-A <sup>488</sup>	25 % Hub-B : 25 % E4-Hub-B	-2	

**Table S3.** SAGE compositions employed in this study. SAGE name, stoichiometries of component hub peptides (defined as the composition), relative surface charge and representative pictograms used in the main text are displayed.



## REFERENCES

- (1) Fields, G. B.; Noble, R. L. *Chem. Biol. Drug Des.* **1990**, 35 (3), 161.
- (2) Fletcher, J. M.; Harniman, R. L.; Barnes, F. R. H.; Boyle, A. L.; Collins, A.; Mantell, J.; Sharp, T. H.; Antognozzi, M.; Booth, P. J.; Linden, N.; Miles, M. J.; Sessions, R. B.; Verkade, P.; Woolfson, D. N. *Science* **2013**, 340 (6132), 595.
- (3) (a) Scholtz, J. M.; Qian, H.; York, E. J.; Stewart, J. M.; Baldwin, R. L. *Biopolymers* **1991**, 31 (13), 1463; (b) Myers, J. K.; Pace, C. N.; Scholtz, J. M. *Biochemistry* **1997**, 36 (36), 10923.
- (4) (a) Schneider, C. A.; Rasband, W. S.; Eliceiri, K. W. *Nat. Methods* **2012**, 9 (7), 671; (b) Schindelin, J.; Rueden, C. T.; Hiner, M. C.; Eliceiri, K. W. *Mol. Reprod. Dev* **2015**, 82 (7-8), 518.
- (5) Sahlin, S.; Hed, J.; Runfquist, I. *J. Immunol. Methods* **1983**, 60 (1-2), 115.